UCRL-16325 errata

University of California

Ernest O. Lawrence Radiation Laboratory

NEUTRON SPECTROSCOPY BY THE USE OF NUCLEAR STARS
FROM 20 TO 300 MeV

TWO-WEEK LOAN COPY

This is a Library Circulating Copy which may be borrowed for two weeks. For a personal retention copy, call Tech. Info. Division, Ext. 5545

Berkeley, California

DISCLAIMER

This document was prepared as an account of work sponsored by the United States Government. While this document is believed to contain correct information, neither the United States Government nor any agency thereof, nor the Regents of the University of California, nor any of their employees, makes any warranty, express or implied, or assumes any legal responsibility for the accuracy, completeness, or usefulness of any information, apparatus, product, or process disclosed, or represents that its use would not infringe privately owned rights. Reference herein to any specific commercial product, process, or service by its trade name, trademark, manufacturer, or otherwise, does not necessarily constitute or imply its endorsement, recommendation, or favoring by the United States Government or any agency thereof, or the Regents of the University of California. The views and opinions of authors expressed herein do not necessarily state or reflect those of the United States Government or any agency thereof or the Regents of the University of California.

UCRL-16325

UNIVERSITY OF CALIFORNIA

Lawrence Radiation Laboratory
Berkeley, California

AEC Contract No. W-7405-eng-48

TO: All recipients of UCRL-16325

FROM: Technical Information Division

Subject: Neutron Spectroscopy by the Use of Nuclear Stars from 20 to 300 MeV.
Please insert the following two pages in report.

ERRATA

"Neutron Spectroscopy by the Use of Nuclear Stars from 20 to 300 MeV," by Rene Remy (M.S. Thesis), August 17, 1965.

Page

iii In the Contents, III.D. the page number should be 23, not 22.

21 On the third line, the reference should be 9, not 12.

23 Eighth and ninth lines should read: Values of R_d are obtained from results of Table XII and are given in Table III for each class.

25 Lines 12 and 13 should read: 3. Each $\overline{z}_i$ is then weighted by a normalized f_i. $f_i(\%) = \frac{N_i(\%)\,\sigma_{in}(\%)}{\sum_i N_i(\%)\,\sigma_{in}(\%)} \cdot 10^2$ (this equation should be added on after the correction f_i as shown here)

27 Table VI, the heading for column 7 should be:
$f_i(\%)$ not f (%)

28 Table VII, the heading for column 7 should be changed as for page 27.

29 Table VIII, same change as 27.

30 Table IX, same change as 27.

31 Table X, same change as 27.

43 7th line from bottom of page should read: % refers to the total number of prongs of the class (i.e. $B_1 + B_2 = 100\%$)

45. Should read: Table XVIII. Number and percentage of stars that had a black track which was rejected as being an unidentified residual nucleus.

63 6th line should read: In that case, our assumptions . . .

66 The reference numbers were changed in the text of UCRL-16325 but were not changed in the list of references. Attached to this errata is a corrected reference list.

REFERENCES

1. M. Goldberger, The Interaction of High-Energy Neutrons and Heavy Nuclei, Phys. Rev. 74, 1269 (1948).
2. R. Serber, The Production of High Energy Neutrons by Stripping, Phys. Rev. 72, 1008 (1947).
3. R. Serber, Nuclear Reactions at High Energies, Phys. Rev. 72, 1114 (1947).
4. V. Weisskopf, Statistics and Nuclear Reactions, Phys. Rev. 52, 295 (1937).
5. K. J. Le Couteur, The Evaporation Theory of Nuclear Disintegration, Proc. Phys. Soc. (London) A63, 259 (1950).
6. Niels Bohr, Neutron Capture and Nuclear Constitution, Nature 137, 344 (1936).
7. Walter Barkas, Nuclear Research Emulsions, Vol. 1 (Academic Press, New York and London, 1963).
8. Walter Barkas (private communication), 1965.
9. Walter Barkas and Martin Berger, Tables of Energy Losses and Ranges of Heavy Charged Particle, NASA SP-3013 (1964).
10. P. Demers, Ionographie - Les Emulsions Nucleaires - Principes et Applications, (Presses Universitaires de Montreal, 1958).
11. William H. Sullivan, Trilinear Chart of Nuclides, (1957), ORNL (no number).
12. L. Evan Bailey, Angle and Energy Distributions of Charged Particles from the High-Energy Nuclear Bombardment of Various Elements (Ph.D. Thesis), UCRL-3334, March 1956.
13. W.D. Lock and P.V. March, A Study of the Nuclear Disintegration Produced by 950-MeV Protons, Proc. Roy. Soc. (London) A231, 368 (1955).
14. William Paul Ball, Nuclear Scattering of 300 MeV Neutrons, UCRL-1938, August 1952.
15. R. Hildebrand, D. Hicks, W. Harker, Summary of Neutron Cross Section Measurements for 14 MeV to 280 MeV Neutrons, UCRL-1305, May 1951.
16. Roger Wallace and Charles Sondhaus, Techniques Used in Shielding Calculations for High-Energy Accelerators: Applications to Space Shielding, UCRL-10436, October 1962.

Research and Development

UCRL-16325

UNIVERSITY OF CALIFORNIA

Lawrence Radiation Laboratory
Berkeley, California

AEC Contract No. W-7405-eng-48

NEUTRON SPECTROSCOPY BY THE USE OF NUCLEAR STARS FROM 20 TO 300 MeV

René Remy

(M. S. Thesis)

August 17, 1965

NEUTRON SPECTROSCOPY BY THE USE OF NUCLEAR STARS FROM 20 TO 300 MeV

CONTENTS

Abstract v

I. Introduction 1

II. Nuclear-Star Method 3

A. Star-Production Process 3

B. Hidden Energy, Visible Energy 4

C. Q Value 6

D. Star-Method Problems 8

E. Assumptions and Approximations. 9

III. Experimental Procedure 11

A. Bombarding Neutron Spectra 11

B. Scanning Method 18

C. Visible-Energy Computation 19

D. Average Q Value. 22

E. Calibration Track. 25

F. Correction Factor. 35

IV. Results. 41

A. Size of Stars and Prong Distribution. 41

B. Average Visible Energy per Star and Its Distribution . . . 44

C. Distribution of Stars in 10-MeV Intervals 52

D. Results for E_n = 20 MeV. 57

V. Conclusions 62

Acknowledgments 65

References 66

NEUTRON SPECTROSCOPY BY THE USE OF NUCLEAR STARS FROM 20 TO 300 MeV

René Remy

Lawrence Radiation Laboratory
University of California
Berkeley, California

August 17, 1965

ABSTRACT

Stars produced in emulsion by incident neutrons of known average energy (E_n) were used to obtain the average visible energy released per star ($\overline{E}_v$) as a function of E_n.

The different neutron average incident energies were 20, 100, 160, 220, and 300 MeV.

Our goal was to find a good way to discriminate among the different E_n's in order that those results could be useful for neutron spectroscopy purposes.

Although a good discrimination was obtained for $\overline{E}_v$ as a function of E_n, real values of $\overline{E}_v$ depend strongly on the validity of one of our working assumptions (average kinetic energy of grey prongs is independent of neutron incident energy).

We found that a much simpler method could be used to reach the same goal--the average number of grey prongs per star offers, in that range of neutron incident energy, a very good discrimination among the different E_n's.

So the use of a simplified method, which consists of counting the number of stars together with the number of grey prongs, should provide a simple way to obtain the average incident neutron energy for an unknown bombarding neutron spectrum in the range 20 to 300 MeV.

I. INTRODUCTION

The use of recoil protons in nuclear emulsion has been quite extensive in the past as a tool in neutron spectroscopy. But when we deal with very energetic neutrons, the length of the recoil proton's track becomes so long that the beginning and end of a track seldom occur in the same emulsion plate. It is always possible to assemble stacks of emulsion and to follow tracks from one emulsion plate to another, but such technique requires a tremendous amount of scanning.

Because energetic neutrons also produce nuclear stars in emulsion, it seems very logical to try to use these stars for neutron-spectroscopy purposes. We may expect that the average kinetic energy of a proton expelled from a nuclear star type disintegration will be less than the average kinetic energy of a recoil proton, given the same energy for the incoming neutron in both cases; in the former case the neutron's kinetic energy must be shared between the different outgoing particles, not only in the form of kinetic energy but also in the form of what we call Q value (Sec. II. C). In addition, the direction of incident neutrons must be known if we are to obtain valid results when recoil protons are used.

Although for the star method we do not need to know the direction of incident neutrons, this method involves other formidable problems not found with the recoil-proton method (Sec. II. D).

This work was an attempt to see if, by using nuclear stars in emulsion, we could obtain some overall results that would be useful in neutron spectroscopy in the energy range from 20 to 300 MeV.

The lower limit (20 MeV) was chosen because for less energetic neutrons (<20) the recoil-proton method is far better than the star method, for the following reasons:

1. For energy less than 20 MeV, the star yield in emulsion becomes too low to provide a good statistic.

2. For a head-on collision between a 20-MeV neutron and a hydrogen nucleus, the range of the proton in Ilford K-5 emulsion is 0.2 cm. A track of this length has a fairly good probability of beginning and ending in the same emulsion plate. This lower limit remains, however, quite arbitrary.

The upper limit (300 MeV) was chosen in order to avoid pion production. Although some pions may be produced with neutron energies around 300 MeV, there are so few that they may be assumed to be non-existent.

We will try, in a rather empirical way, to answer crudely the question, "What average proportion of the total incoming energy appears in visible form, and in invisible form, as a function of the incoming neutron energy ?"

II. NUCLEAR-STAR METHOD

A. Star-Production Process

In standard nuclear emulsion, the nuclei may be roughly classified as "light-nuclei group" or "heavy-nuclei group." The light-nuclei group includes H, C, N, O, and S. The heavy-nuclei group includes Ag, Br, and I. The nuclei of all these elements, except H, when hit with sufficient energy by a particle, may produce what is called a nuclear star.

Let us assume for convenience that the incoming particle is a nucleon. When the nucleon penetrates into the nucleus it may bring enough energy to break that nucleus apart. This is a process in which every possible mode of disintegration becomes possible, provided the incoming energy is sufficient. Each of these modes is an inelastic process occurring when a threshold energy is passed. When the incoming nucleon brings energy greater than the total binding energy of the target nucleus, every mode of disintegration becomes possible (excluding strange-particle production).

It is generally assumed that two processes are involved in the star-type disintegration. The theory of the first, a mechanism known as "nuclear cascade," was developed by Goldberger[1] from Serber's model.[2,3] In this process part of the energy available is received by one or more particles which are inside the nucleus but which come out. The main features of that process are that these particles are strongly peaked in the forward direction (with respect to the incoming nucleon's direction), and that their energy may range from near that of the incident nucleon to below a few MeV.

After the first process has taken place, the residual nucleus consists of an excited intermediate nucleus, which will evaporate enough particles to ensure at least quasi-stability for the residual nucleus. The theory of this second process, known as the "evaporation process," was developed by Weisskopf[4] and Le Couteur,[5] who used Bohr's[6] theory of the compound nucleus.

For a given star it is, however, possible to have only one of these two processes: no evaporation particle (all energy carried away by cascade particles), no cascade particle (all energy available becomes excitation energy for the intermediate nucleus).

B. Hidden Energy, Visible Energy

Whenever a charged particle travels through an emulsion, it leaves a track that becomes visible after processing. For a given particle and a given emulsion, a one-to-one relationship exists between the range and the kinetic energy of the particle. This range-energy relationship has been investigated and computed by Barkas,[7,8] Barkas and Berger,[9] and Demers,[10] among several others, for several kinds of particles and emulsions.

By means of these range-energy tables we can determine the kinetic energy of a particle at the beginning of its track, provided that we know (a) the type of particle, (b) the properties of the emulsion used, and (c) that the track begins and ends in the emulsion. In these range-energy tables, two identical particles with the same kinetic energy in the same medium were assumed to have the same range. Although this is not necessarily true, it is a fair assumption statistically.

Unfortunately, neutral particles, such as neutrons and gamma rays, are not directly detectable in nuclear emulsion. The only way they can be detected is by means of recoil protons (resulting from elastic collisions with hydrogen nuclei) or nuclear stars (formed by disintegration of nuclei heavier than hydrogen).

The probability that a neutral particle outgoing from a star-type disintegration will produce a second detectable reaction near enough to the first one to permit correlation between the two events may be considered as being zero. Even if such a rare event occurs, the presence of many recoil-proton tracks and the absence of a visible link between the two events makes them impossible to correlate.

Let us analyze what is going on when a star is produced in a nuclear emulsion. We do not distinguish between the cascade process and the evaporation one, as we are interested only in the total energy balance. When we speak of an incoming nucleon without explicitly specifying its nature, we mean a neutron. Suppose that an incoming neutron with kinetic energy E_n hits a nucleus C (which is supposed to be at rest) and produces a disintegration such as

$$n + C \rightarrow p\,A_i + qB_i + D, \qquad (1)$$

in which A_i = charged particle (see assumption 7, Sec. II. E)

B_i = neutral particle

D = residual nucleus

p and q = any numbers.

Let Q_t be the threshold energy necessary for reaction (1) to occur. If $E_n > Q_t$, we may write

$$E_n = E + Q_t. \tag{2}$$

(Strictly speaking, the total energy brought in by the neutron may be greater than E_n, because in some cases it must include the mass energy equivalence of the amount of mass of the incoming neutron that was transformed in kinetic energy. This is the case when no free neutrons are among the outgoing particles.) With E the energy available to be shared between the different outgoing particles in the form of kinetic energy, and with the assumption that D is left in an unexcited state, Eq. (2) may be written

$$E_n = \sum_{i=1}^{m} E_i + Q_i, \tag{3}$$

with $m = p + q + 1$

E_i = kinetic energy of outgoing particle i.

Q_i = Q value associated with outgoing particle i (see Sec. II. C).

We have, of course,

$$E = \sum_{i=1}^{m} E_i \tag{4}$$

$$Q_t = \sum_{i=1}^{m} Q_i . \tag{5}$$

From the above only

$$E_v = \sum_{i=1}^{p+1} E_i + Q_i \tag{6}$$

may appear in a visible form with $p + 1$ = charged particles + residual nucleus. If every $(p + 1)$ charged particle could be easily identified and if every $(p + 1)$ track ended in the emulsion, there should be no great problem to find E_v.

Let us, however, exclude the residual nucleus from our balance of visible energy, for reasons that are apparent later on (see assumption 8, Sec. II. E).

We define

$$\text{visible energy} = E_v = \sum_{i=1}^{p} E_i + Q_i \tag{7}$$

$$\text{hidden energy} = E_h = \sum_{i=p+1}^{m} E_i + Q_i \tag{8}$$

with, of course,

$$E_n = \sum_{i=1}^{p} E_i + Q_i + \sum_{i=p+1}^{m} E_i + Q_i = E_v + E_h. \tag{9}$$

C. Q Value

In order for a certain type of disintegration to occur, the incoming nucleon must bring enough energy to satisfy the mass-energy equivalence balance. This type of reaction is called "threshold reaction," and that threshold energy is what we call the Q_t value of the reaction.

The way we have defined Q_t in the previous equations shows that when $Q_t > 0$, then E_n must be $\geq Q_t$ for the reaction to occur. When $Q_t < 0$, we have $E = -Q_t$ when $E_n = 0$. This means that even with zero kinetic energy of the incoming neutron, some energy E will be available as kinetic energy of the outgoing particle. However, a negative Q_t cannot occur for reactions such as those we consider in assumption 1 (see Sec. II. E). Once a mode of disintegration is identified, Q_t may be computed by means of the following equation.

$$Q_t = (A - B)\,\alpha \tag{10}$$

with $A = \sum_{i=1}^{m} M_i$ [M_i = mass of ith outgoing particle in amu (Ref. 11)]

m as defined in Eq. (3)

B = mass of the target nucleus in amu (Ref. 11)

$\alpha = 931.162 \frac{\text{MeV}}{\text{amu}}$.

Now the question is how to find the Q_i's in Eq. (5). In other words, What Q value should be associated with each outgoing particle? To find the Q value of a particle A, we use the following equation:

$$Q_A = (a + b)z - (M_a + M_b - M_A) \tag{11}$$

with

a = number of neutrons in particle A

b = number of protons in particle A

z = binding energy per nucleon in the target nucleus as defined by Eq. (12).

M_a = mass energy equivalence of a unbound neutrons

M_b = mass energy equivalence of b unbound protons

M_A = mass energy equivalence of particle A when unbound.

In Eq. (11), only z is a function of the target nucleus. Thus for a given outgoing particle A, the term $(M_a + M_b - M_A)$ is a constant for every possible kind of target nucleus. In fact, this term is simply the total binding energy of the (a + b) nucleons in particle A, when this particle is considered a free particle. Once the target nucleus is known and A is identified, Q_A may be computed, provided we have an expression for z (x) (with x = identity of the target nucleus variable).

Two cases must be considered in order to fit Eqs. (5) and (10).

1. A reaction in which there are no outgoing neutrons.
   Example: $^{12}C + n \rightarrow t + 5d$ (see assumption 7, Sec. II.E, for explanation of symbols used).
2. A reaction in which there is at least one outgoing neutron.
   Example: $^{12}C + n \rightarrow 3\,\alpha + n$ (this type of reaction corresponds to our assumption 1)

For type 2 reaction, we have

$$z\,(x) = \frac{A - B}{C}, \tag{12}$$

with A = mass energy equivalence of the C nucleons in the target nucleus x

B = mass energy equivalence of target nucleus x

C = number of nucleons in target nucleus x.

For reactions of type 1 above, Eq. (12) becomes

$$z^{*}(x) = \frac{A - B}{C^{*}} \tag{13}$$

with

C^{*} = number of nucleons of target nucleus x plus one (the incoming neutron).

Equations (11), (12), or (13), are quite general and permit computation of the Q_i's of every kind of particle.

D. Star-Method Problems

When we try to use nuclear-star production in emulsion for neutron spectroscopy purposes, we are faced with some serious problems, among which the main ones are:

1. No monoenergetic neutrons can be obtained in that range of energy (20 to 300 MeV).

2. It is almost impossible to tell what the target nucleus was and therefore to identify the reaction.

3. To identify the nature of the particle for a given track requires careful and very long measurements. It is only when the particle ends in the emulsion and has a long range that it may be identified fairly accurately. For particles with a charge greater than 2, the track is usually so small that no identification is possible.

4. Some of the tracks will not end in the emulsion, and the probability for this occurring is greater for fast particles than for slow ones.

5. The results that can be obtained have only a statistical meaning, and with the devices now available this means a tremendous amount of scanning work. The accuracy of the results depend strongly on the skill and freshness of the scanner.

Some partial solutions to these problems have already been found or are now under investigation. Among these are:

1. The bombardment of targets with protons and deuterons gives a fairly peaked neutron spectrum that is theoretically symmetric about the peak, so that the neutrons may be considered as being monoenergetic and having the energy of the peak. Some theoretical predictions are made by Serber's stripping theory.[2]

2. Some criteria are used to classify the target nuclei into light-nuclei group (C, N, O, S) and heavy-nuclei group (Ag, Br, I).[12,13]

3. Particles can be identified by means of gap counting, blob counting, and delta rays.[7,10] Some new ways that may provide automatic identification, now under investigation at the Lawrence Radiation Laboratory, are T. V. scope and measurement of track width.

4. Even for a particle not stopping in the emulsion, a good estimation of its kinetic energy can be obtained by blob or gap counting at each end, provided that the track in the emulsion is long enough.

5. Some semiautomatic devices already exist and more extensive prospects are under investigation.

E. Assumptions and Approximations

During this work, we made the following working assumptions and approximations:

1. Each star is produced by an inelastic-type reaction (at least one outgoing neutron).

2. We replaced the symmetric neutron spectra (given by Serber's stripping theory[2] or by Ball[14]) with monoenergetic neutrons having the energy of the peak of the spectrum (see Sec. III. A).

3. The range of each track is approximated by the straight line connecting its beginning and its end, and straggling of the particle is not accounted for.

4. The kinetic energy of each track not ending in the emulsion is estimated from a calibration track (see Sec. III. E).

5. No attempt to distinguish between light-nuclei group and heavy-nuclei group is made.

6. The proportion of inelastic collisions not producing a star-type reaction remains a constant percentage of the total inelastic cross section for each isotope and for each energy.

7. All visible tracks are assumed to belong to the "singly-charged-particle group" or the "doubly-charged-particle group." The particles that we assume to be possible visible outgoing particles are the following:

Particle	Symbol
proton	p
deuteron	d
triton	t
helium-3	a
helium-4	α
lithium 8	^{8}Li (hammer track)
unknown residual nucleus	D

8. When a star has a very black and very short prong (less than 10 microns), this prong is rejected as being made by an undetermined residual nucleus.

9. Each star, unless it is doubtless a proton star, or an α star, is assumed to be a neutron star. By doubtless a proton star, we mean:

a. An event in which one of the prongs goes from black at the center of the star to grey at the end of the prong.

b. An event in which a prong, having the same class all along its range, suddenly disappears inside the emulsion.

The α stars are produced by α emitters, such as impurities (thorium C) that are unavoidable components of the emulsion. We considered as α stars, and thus rejected, all the stars fulfilling the three following conditions:

a. All the prongs are black.

b. All the prongs have a length of 50 microns or less.

c. The difference in length of all the prongs of a given star is not more than 10 microns.

10. Only events with two visible prongs (excluding residual nucleus) will be considered to be true stars.

11. The value of R_d [see Eq. (20)] depends only on the class of the prong at its exit point and not on the neutron incident energy. (This implies that the average energy of black-grey, grey-black, and grey prongs is independent of the neutron incident energy.)

III. EXPERIMENTAL PROCEDURE

A. Bombarding Neutron Spectra

Six different Ilford K-5 emulsions (3 inch × 1 inch × 600μ) were bombarded under different conditions (see Table I).

According to assumption 2 (Sec. II. E), the neutrons were considered to be monoenergetic and to have the energy of the peaks as given in Figs. 1 through 5.

As may be seen in Table I, five emulsions were bombarded with neutrons obtained from stripping of deuterons by a Be target.

According to Serber's stripping theory,[2] we have

$$P(E)dE = \frac{(\Sigma_d E_d)^{1/2}}{\pi \left[(E - \frac{1}{2} E_d)^2 + \Sigma_d E_d\right]} dE, \tag{14}$$

with Σ_d = binding energy of deuteron = 2.18 MeV

E_d = deuteron's incident energy

$P(E)dE$ = probability that neutron is in energy range dE.

Such neutron distribution peaks at

$$E_n = \frac{1}{2} E_d . \tag{15}$$

This E_n corresponds to the value taken into account in assumption 2.

The theoretical spectrum has also a half width (full width at half maximum) given by

$$\Delta E_{1/2} = 2 (\Sigma_d E_d)^{1/2} \tag{16}$$

and is symmetrical about the peak.

Figures 1 through 4 show the neutron spectra predicted on the basis of Serber's theory.

Emulsion number 5 was bombarded with neutrons of 300-MeV obtained by bombarding a Be target with 360-MeV protons, because the highest energy available in the 184-inch cyclotron for incident deuterons on Be targets is too low to yield 300-MeV neutrons from stripping. Figure 5 shows the aspect of the bombarding neutron spectrum for E_n = 300 MeV as obtained by Ball.[14]

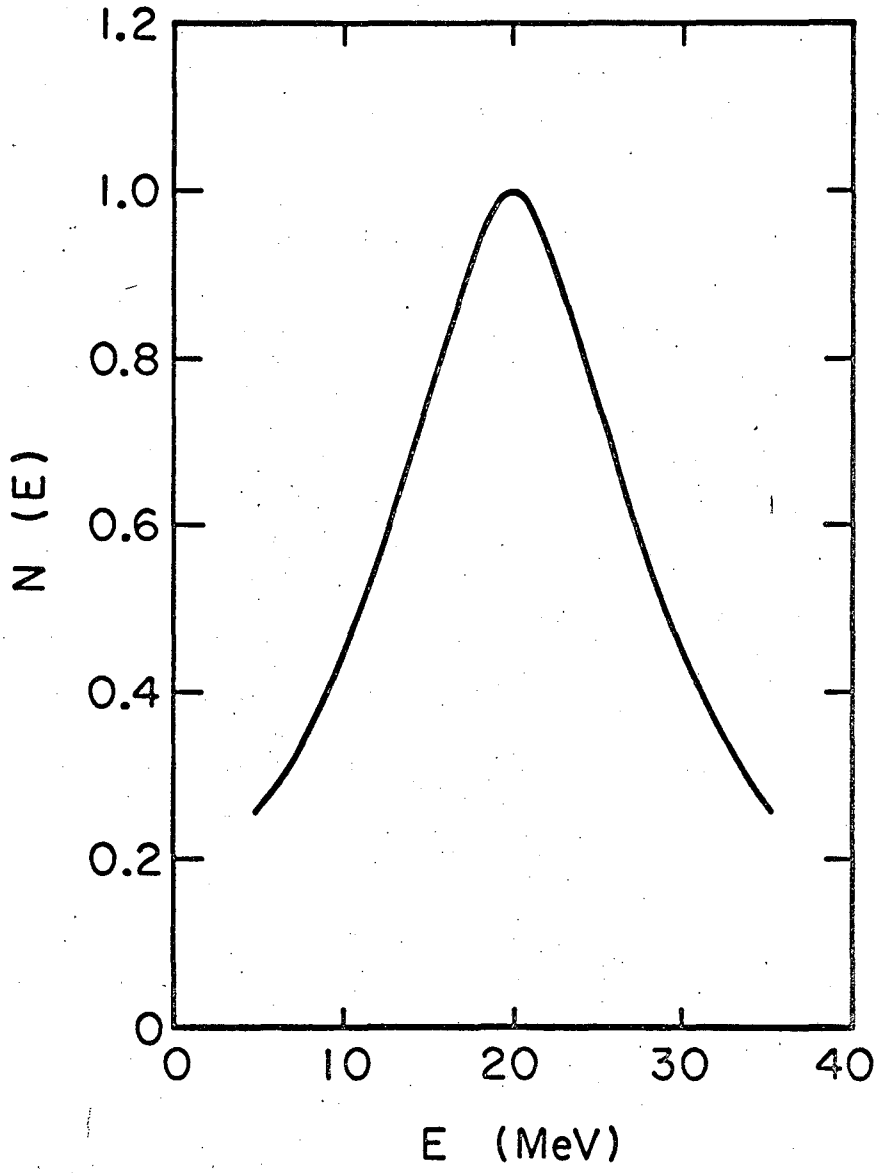

MU-36549

Fig. 1. Plot of equation 14 after normalization with E_d = 40 MeV; E_n = 20 MeV. Neutron spectrum as predicted by Serber's theory.

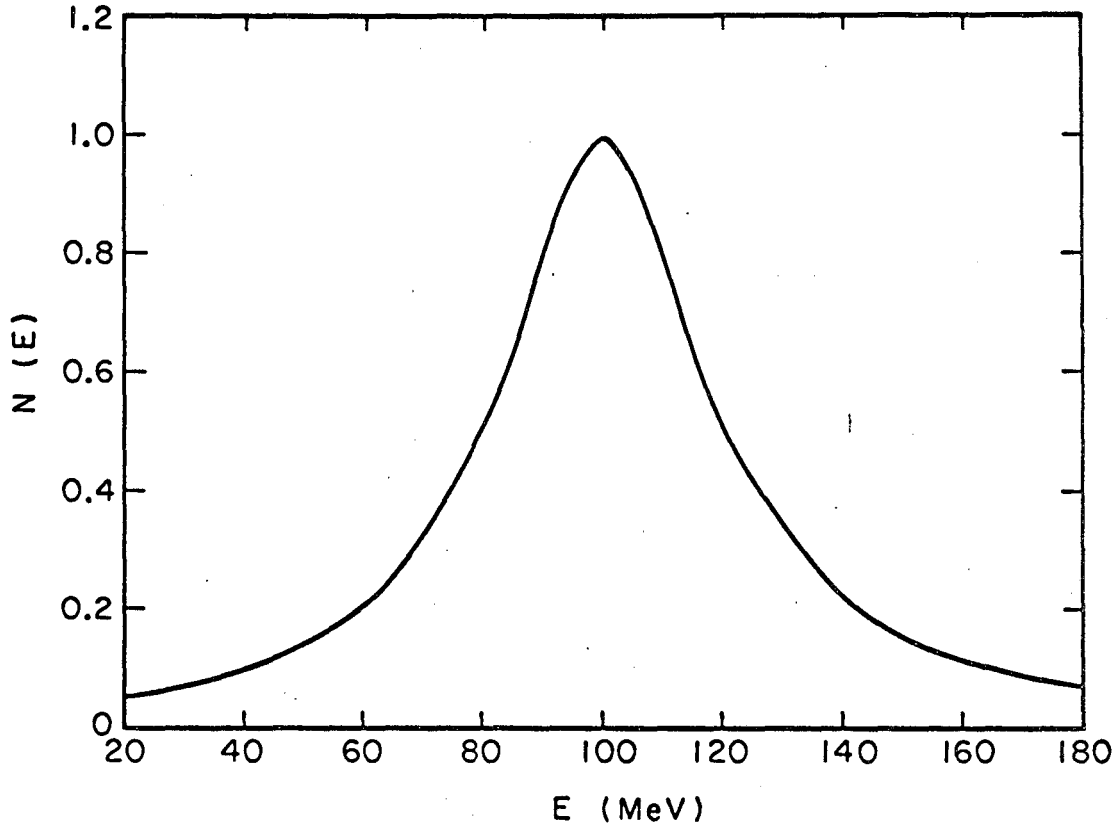

MU-36547

Fig. 2. Plot of equation 14 after normalization with E_d = 200 MeV; E_n = 100 MeV. Neutron spectrum as predicted by Serber's theory.

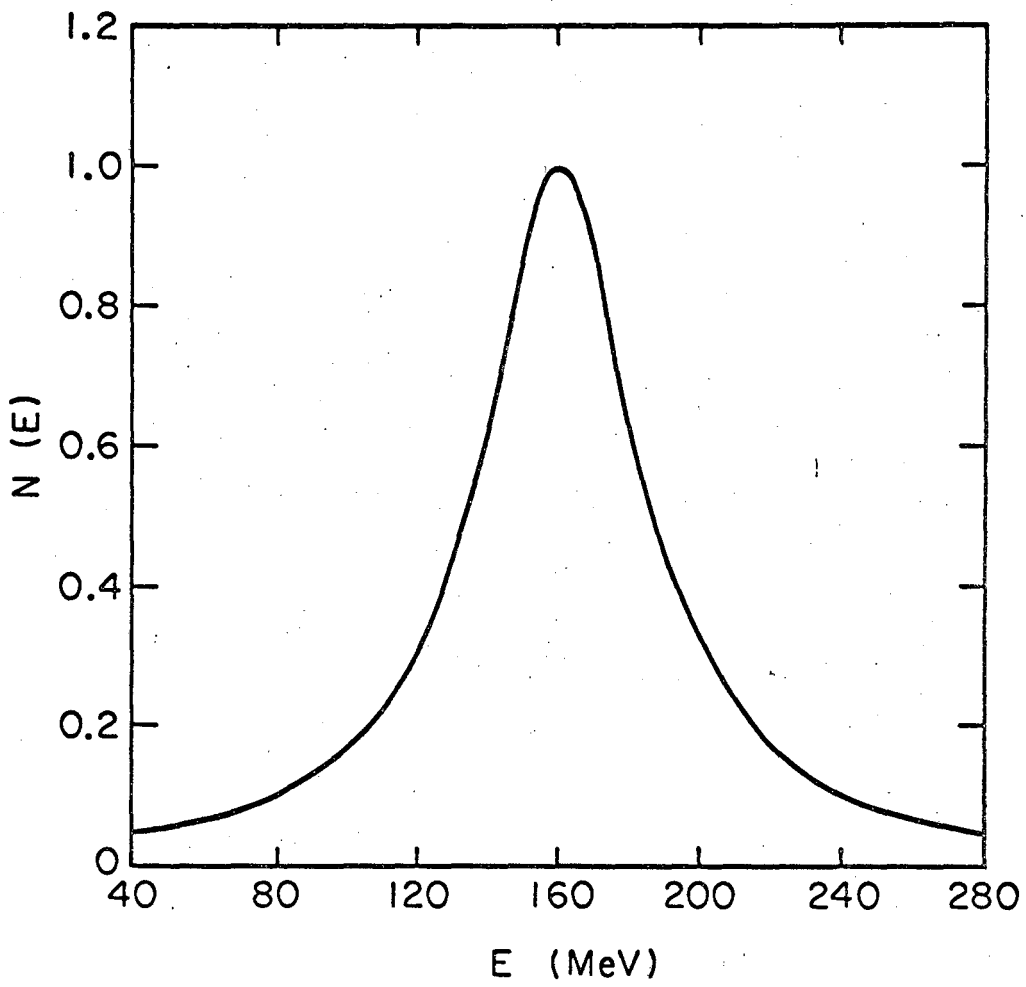

MU-36548

Fig. 3. Plot of equation 14 after normalization with E_d = 320 MeV; E_n = 160 MeV. Neutron spectrum as predicted by Serber's theory.

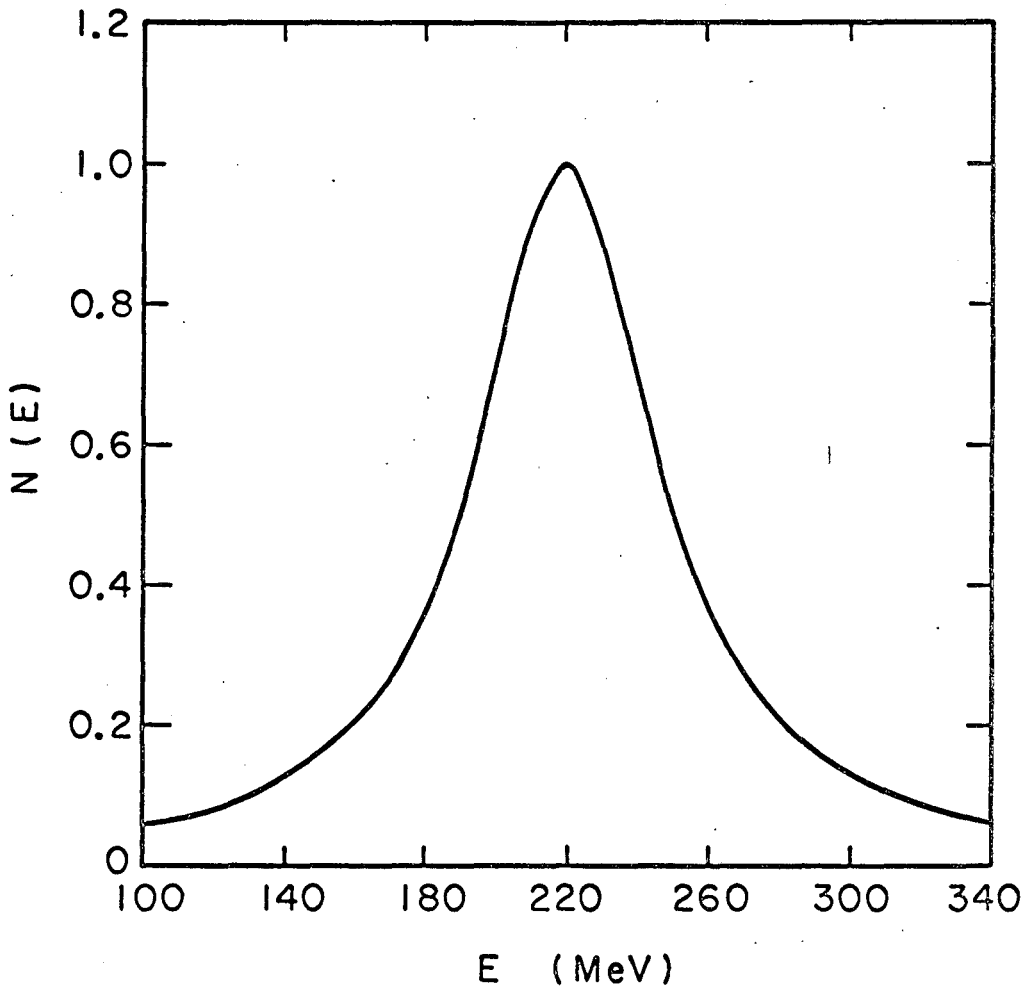

MU-36550

Fig. 4. Plot of equation 14 after normalization with E_d = 440 MeV; E_n = 220 MeV. Neutron spectrum as predicted by Serber's theory.

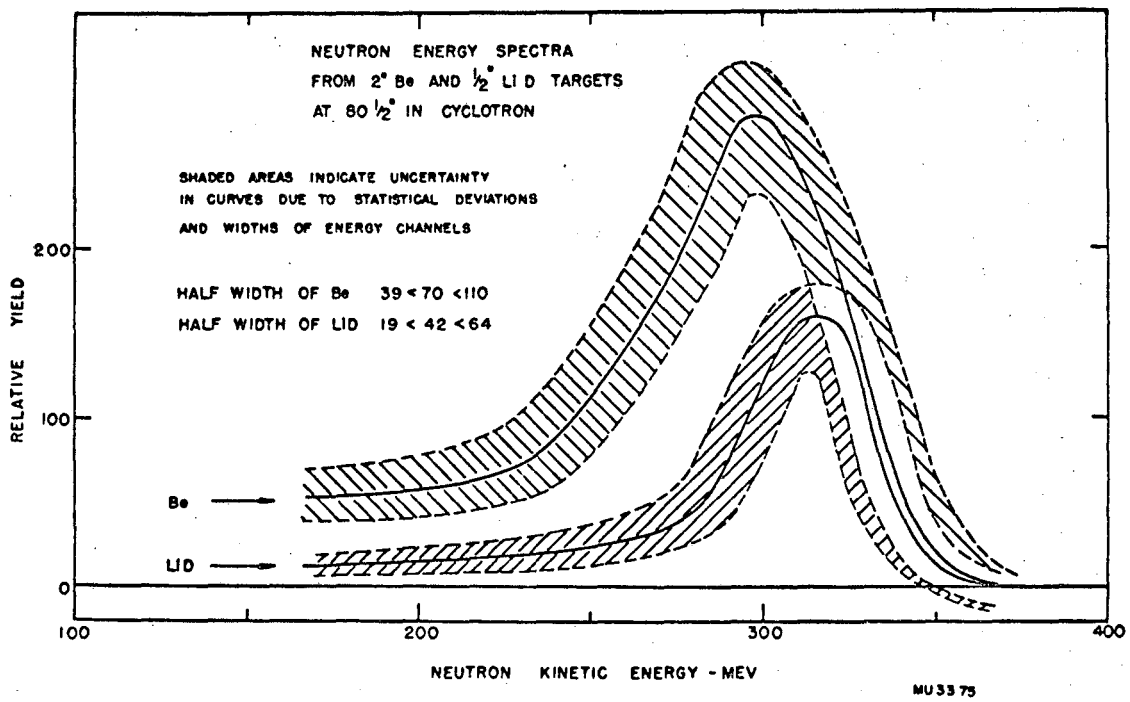

Fig. 5. Neutron spectrum for E_n = 300 MeV as determined by Ball.[14] The upper curve applies to this experiment.

Table I. Chart of bombardment of the emulsions.

Emulsion No.	Bombarding particle	Target	Neutron energy (MeV)	Accelerator used
0	deuterons	Be	20	88-inch cyclotron
1	deuterons	Be	220	184-inch cyclotron
2	deuterons	Be	220	184-inch cyclotron
3	deuterons	Be	100	184-inch cyclotron
4	deuterons	Be	160	184-inch cyclotron
5	protons	Be	300	184-inch cyclotron

B. Scanning Method

More than 500 stars were scanned at random in each emulsion plate. The number of prongs on each star were counted and each prong was classified according to the following criteria.

Class	Criteria
Black	<10 gaps in the field of view (100 microns)[a]
Black-grey	10 to 20 gaps in the field of view
Grey-black	21 to 50 gaps in the field of view
Grey	>50 gaps in the field of view

a. The number of gaps were counted in the field of view (100 microns of projected length) so that the error made in counting gaps in track having a great dip angle is more or less compensated for.

These classes were given at the beginning of each prong (center of the star). Each prong was then individually followed to its end or exit point.

If the prong ended in the emulsion, the three coordinates of its end and beginning points were recorded on IBM cards; the range scope from the Lawrence Radiation Laboratory, Berkeley, were used.

If the prong did not end in the emulsion, a class was also determined at the exit point, then each point (beginning and exit) recorded on IBM cards.

Stars having their center on the edge of the emulsion plate were rejected, because it was not possible to know if we missed one or more prongs going in the wrong direction. For each star the following information was recorded on IBM cards.

General information per star

number of the emulsion
number of the star scanned
total number of prongs of the star
one black track rejected as being residual nucleus, or no such black track

Information per prong

prong number

prong class at the center of the star

prong ending in emulsion or continuance beyond emulsion

prong class at the exit point (for prong not ending in the emulsion)

coordinates of beginning and end points

C. Visible-Energy Computation

Once the three coordinates of the beginning and end points were known, the range of the particle could be computed on the basis of the following equation.

$$R_i = [S_x^{\,2} (x_i - x_{i-1})^2 + S_y^{\,2} (y_i - y_{i-1})^2 + S_z^{\,2} (z_i - z_{i-1})^2]^{1/2} \qquad (17)$$

with x_i, y_i, z_i = coordinates of point i

x_{i-1}, y_{i-1}, z_{i-1} = coordinates of point i-1

S_x = shrinkage factor in x direction

S_y = shrinkage factor in y direction

S_z = shrinkage factor in z direction.

The total range is then given by

$$R_T = \sum_{i=1}^{n} R_i$$

with x_0, y_0, z_0 = coordinates of end point

x_n, y_n, z_n = coordinates of beginning point.

In our case, Eq. (17) reduced to (see assumption 3)

$$R_T = [(x_1 - x_0)^2 + (y_1 - y_0)^2 + S^2 (z_1 - z_0)^2]^{1/2}. \qquad (18)$$

Because the emulsion was mounted on a glass plate before processing, we have

$$S_x = 1, \qquad S_y = 1, \qquad S_z = S .$$

Table II gives the values of S for the six different emulsion plates used.

Table II. Values of shrinkage factor for emulsion bombarded with neutrons of energy E_n.

Emulsion number	E_n (MeV)	Shrinkage factor
0	20	2.05
1	220	2.11
2	220	2.40
3	100	2.02
4	160	2.03
5	300	2.11

From the range of a prong that stops in the emulsion, its kinetic energy was computed from tables similar to those given by Barkas and Berger.[12]

Two cases were considered:

1. Prongs ending in the emulsion: Let us assume for the moment that we have identified the particle. The total energy taken away by this particle is

$$E = E_k + Q \tag{19}$$

with

E_k = kinetic energy

Q = average Q value associated with the given particle (see Sec. III. D).

2. Prongs not ending in the emulsion: To reject all prongs not stopping in the emulsion seemed at first an obvious thing to do. But in doing so we would miss a much greater proportion of prongs from fast particles than from slow ones. Also, the probability for a many-pronged star to have at least one prong not stopping in the emulsion is greater than for a two-pronged star. To obtain even an estimation of such probabilities requires very complicated computations. So we decided not to reject stars on the basis of their prongs not stopping in the emulsion. The kinetic energy for such prongs was arbitrarily estimated in the following way:

a. If the prong changes its class before leaving the emulsion. To the actual range in the emulsion we arbitrarily add a residual range, and then compute the kinetic energy from this fictitious total range. This residual range is given by

$$R_d = \frac{R_1 + R_2}{2} , \tag{20}$$

with R_1 = residual range of the recoil proton at the point on the calibration track chosen as the beginning point of the same class as the scanned prong at its exit point.

R_2 = residual range of the recoil proton at the point chosen on the calibration track as the end point of the same class as the scanned prong at its exit point. (see Table III and Table XII).

Table III. Value of residual range to be added for prongs not ending in the emulsion.

Class[b]	Residual range (μ)[a]				
	E_n = 20 MeV	E_n = 100 MeV	E_n = 160 MeV	E_n = 220 MeV	E_n = 300 MeV
Black	400	400	400	400	400
Black-grey	785	785	785	785	785
Grey-black	3 575	3 575	3 575	3 575	3 575
Grey	11 780	11 780	11 780	11 780	11 780

a. E_n is the bombarding neutron's energy.

b. "Class" refers to the class of the prong at its exit point.

Equation (20) means: (a) that the residual range R_d is obtained from the calibration track; (b) that for a given class the value of R_d taken into account is the length between the stopping point of the recoil proton and the point which is the middle of the portion of the calibration track defined as belonging to that given class; (c) the class selected to obtain the value of R_d is the class of the scanned prong in 100 microns (projected length for track's stopping) nearest the point where the particle track leaves the emulsion. Values of R_d are obtained for results of Table X and are given in Table XII for each class.

b. <u>If the prong does not change its class before leaving the emulsion.</u>

1. The track is grey, grey-black, or black-grey.
   A residual range similar to that defined in Eq. (20) is arbitrarily added to the scanned range. The kinetic energy is then computed from the total fictitious range so obtained.
2. The track is black.
   To the scanned range is added a residual range $\overline{R}$, defined as the average length of all black tracks that stopped in the same emulsion plate. We have

$$R_T = R_S + \overline{R} \tag{21}$$

with R_S = scanned range

$$\overline{R} = \frac{\sum_{i=1}^{n} R_i}{n} \tag{22}$$

R_i = ith range of black-tracks that stop and were scanned in the same emulsion plate.

Table IV gives values of $\overline{R}$ for the different emulsions.

D. Average Q Value

Equations derived in Sec. II. C permit computation of the Q_i's, once the target nucleus is known. As we have already pointed out, there is no known way to identify the target nucleus.

Remember that Eq. (11) is of the form

$$Q_i = nz - C,$$

Table IV. Values of $\overline{R}$ (average range of black track) in emulsion bombarded with neutrons of energy E_n.

Emulsion number	E_n (MeV)	$\overline{R}$ (μ)
0	20	40
1	220	141
2	220	179
3	100	128
4	160	151
5	300	138

in which n and C are functions of i only (the identity of the outgoing particle), and z is a fuction of the target nucleus only. Let us modify Eq. (11) in the following way

$$\bar{Q}_i = n\bar{z} - C, \tag{23}$$

in which $\bar{z}$ is the value of z averaged for the whole emulsion.

The term $\bar{z}$ is obtained as follows:

1. From Eq. (12), z is computed for each isotope present in the emulsion (except hydrogen).
2. For a given atom we obtained $\bar{z}_i$ by weighting the z of its naturally occurring isotopes by its percentage of abundance (see Table V).
3. Each $\bar{z}_i$ is then weighted by a normalized N_i and a normalized σ_{in}.

   N_i = number of atoms of specie i for unit volume of emulsion.

   σ_{in} = inelastic cross section of atoms of specie i for energy E_n. (See Tables VI through X) (Ref. 15)

Now $\bar{z}$ is no more a function of the target nucleus, but it becomes a function of E_n. The term $[\bar{z}(E_n)]$ is identical to $\bar{Q}(E_n)$ for protons, as given in Table XI.

The $\bar{Q}_i(E_n)$ as obtained from Eq. (23) are given in Table XI.

E. Calibration Track

The longest recoil-proton track ending in the emulsion was chosen as the calibration track (see Fig. 6). This track, found in emulsion 4 (E_n = 160 MeV), had a total length of 1.7 cm, which corresponds to a proton with an energy of 70 MeV. This track was followed and several portions of it were recorded on IBM cards.

From this information we obtained the data given in Table XII, which permitted the computation of the residual ranges R_d of Eq. (20) (see Table III).

Several other recoil-proton tracks were also followed in the other emulsions and were found to be, within acceptable limits, identical to the calibration track. The calibration track from which the class criteria of Sec. III. B were derived was accepted as valid for all six emulsions.

Table V. Nuclei and isotopes found in emulsion, percentage of natural abundance, z per isotope [from Eq. (12)], $\bar{z}_i$ per kind of nucleus.

Nuclei	Isotope	Abundance %	z (MeV)	$\bar{z}_i$ (MeV)
Silver	^{107}Ag	51.82	8.555	8.856
	^{109}Ag	48.18	9.180	
Bromine	^{79}Br	50.54	8.687	8.690
	^{81}Br	49.46	8.694	
Iodine	^{127}I	100	8.445	8.445
Carbon	^{12}C	98.89	7.680	7.678
	^{13}C	1.11	7.470	
Nitrogen	^{14}N	99.63	7.476	7.477
	^{15}N	0.37	7.700	
Sulfur	^{32}S	95.00	8.493	8.496
	^{33}S	0.76	8.499	
	^{34}S	4.22	8.584	
	^{36}S	0.014	8.577	
Oxygen	^{16}O	99.759	7.976	7.975
	^{17}O	0.037	7.750	
	^{18}O	0.204	7.768	

Table VI. Values of $\bar{z}$ for energy of neutrons E_n = 20 MeV.

Nucleus	N_i (10^{20} atoms/ml)	N_i (%)	σ_{in}(barn)	σ_{in} (%)	$\bar{z}_i$ (MeV)	f (%)	$\bar{z}$ (MeV)
Ag	101.01	21.570	0.562	22.25	8.856	36.04	
Br	100.41	21.44	0.465	18.41	8.690	29.64	
I	0.565	0.12	0.585	23.16	8.445	0.21	
C	138.30	29.53	0.180	7.13	7.678	15.81	8.44
N	31.68	6.76	0.202	8.00	7.477	4.06	
S	1.353	0.29	0.300	11.87	8.496	0.26	
O	94.97	20.28	0.232	9.18	7.975	13.98	

Table VII. Values of $\bar{z}$ for energy of neutrons E_n = 100 MeV.

Nucleus	N_i (10^{20} atoms/ml)	N_i (%)	σ_{in}(barn)	σ_{in}(%)	$\bar{z}_i$ (MeV)	f (%)	$\bar{z}$ (MeV)
Ag	See Table VI	See Table VI	1.14	24.73	See Table VI	40.59	
Br			1.00	21.69		35.39	
I			1.26	27.34		0.25	
C			0.22	4.77		10.72	8.54
N			0.25	5.42		2.79	
S			0.44	9.54		0.21	
O			0.30	6.51		10.05	

Table VIII. Values $\bar{z}$ for energy of neutrons E_n = 160 MeV.

Nucleus	N_i (10^{20} atoms/ml)	N_i (%)	σ_{in}(barn)	σ_{in} (%)	$\bar{z}_i$ (MeV)	f (%)	$\bar{z}$ (MeV)
Ag	See Table VI	See Table VI	0.91	25.85	See Table VI	43.09	
Br			0.72	20.45		33.88	
I			1.01	28.69		0.26	
C			0.16	4.55		10.39	8.55
N			0.19	5.40		2.82	
S			0.32	9.09		0.20	
O			0.21	5.97		9.36	

Table IX. Values of $\bar{z}$ for energy of neutrons E_n = 220 MeV.

Nucleus	N_i (10^{20} atoms/ml)	N_i (%)	σ_{in}(barn)	σ_{in} (%)	$\bar{z}_i$ (MeV)	f (%)	$\bar{z}$ (MeV)
Ag	See Table VI	See Table VI	0.88	25.96	See Table VI	43.80	
Br			0.70	20.65		34.63	
I			0.98	28.91		0.27	
C			0.14	4.13		9.54	8.57
N			0.17	5.01		2.65	
S			0.33	9.74		0.22	
O			0.19	5.60		8.89	

Table X. Values of $\bar{z}$ for energy of neutrons E_n = 300 MeV.

Nucleus	N_i (10^{20} atoms/ml)	N_i (%)	σ_{in}(barn)	σ_{in} (%)	$\bar{z}_i$ (MeV)	f (%)	$\bar{z}$ (MeV)
Ag	See Table VI	See Table VI	1.23	25.95	See Table VI	43.65	
Br			0.98	20.68		34.57	
I			1.37	28.90		0.27	
C			0.20	4.22		9.72	8.57
N			0.23	4.85		2.56	
S			0.46	9.70		0.22	
O			0.27	5.70		9.01	

Table XI. $\bar{Q}$ values for different particles as a function of E_n.

Particle	Symbol	E_n (MeV)	$\bar{Q}$ (MeV)	C (MeV) (Eq. 23)	n (Eq. 23)
Proton	p	20	8.44		
		100	8.54		
		160	8.55	0	1
		220	8.57		
		300	8.57		
Deuteron	d	20	14.66		
		100	14.86		
		160	14.88	2.22	2
		220	14.92		
		300	14.92		
Triton	t	20	16.84		
		100	17.14		
		160	17.17	8.48	3
		220	17.23		
		300	17.23		
Helium-3	a	20	17.60		
		100	17.90		
		160	17.93	7.72	3
		220	17.99		
		300	17.99		
Helium-4	α	20	5.47		
		100	5.87		
		160	5.91	28.29	4
		220	5.99		
		300	5.99		
Lithium-8	^{8}Li	20	26.24	41.28	8
		100	27.04		
		160	27.12		
		220	27.28		
		300	27.28		

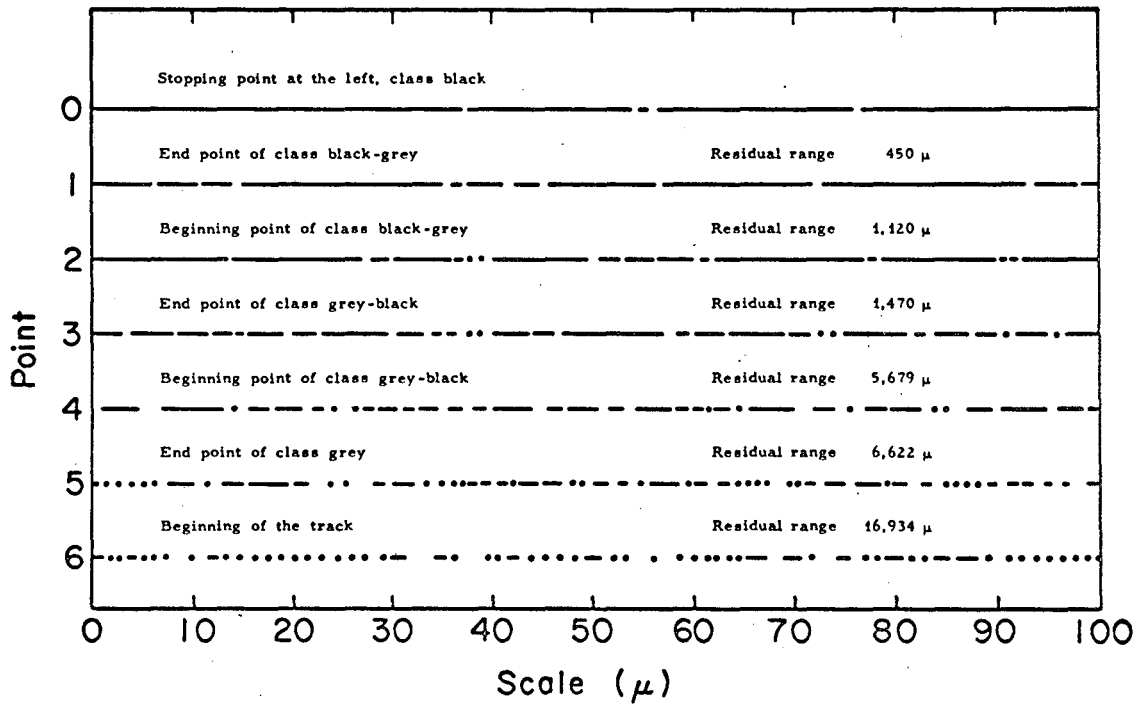

MU-36538

Fig. 6. Calibration track (recoil proton with 70-MeV kinetic energy found in emulsion 4).

Table XII. Range and energy of different points of the calibration track.[a,b,c,d,e]

Point No.	Range (μ)	Energy (MeV)	Class	Eq. (20)
0	----	----	black	
1	455	8.83	black-grey	R_1
2	1127	14.99	black-grey	R_2
3	1471	17.47	grey-black	R_1
4	5679	37.83	grey-black	R_2
5	6621	41.27	grey	R_1
6	16933	70.43	grey	R_2

a. Point numbers are the same as those given on Fig. 6.

b. Range refers to the length between the point in question and the proton's stopping point (point 0).

c. Energy refers to the energy left to the proton at the given points.

d. Last column refers to symbol used in Eq. (20). In each specific case, the choice of R_1 and R_2 depends on the class of the scanned prong at the location where it leaves the emulsion.

e. Class (a) refers to the class of a scanned prong at a point where it leaves the emulsion (to be taken into account in the calculation of values of R_1 and R_2); (b) limits points of the portion of the calibration track defined as having that class.

F. Correction Factor

In a first approximation, all prongs except hammer tracks (^{8}Li) were assumed to be from protons. The results obtained with such an approximation are referred to as "unmodified results." In order to take into account the fact that some of the prongs were actually deuterons (d), tritons (t), helium-3 (^{3}He) or alpha (α) particles, the results were then corrected and then referred to as modified results. Correction was done in the following way:

From experimental and theoretical data,[16] the number of protons, deuterons, tritons, helium-3, and α's to be expected from neutron stars has been crudely estimated. After these data were properly weighted, and the composition of the emulsion and the inelastic cross section were taken into account, the relative proportions of these particles, as given in Table XIII, were obtained.

Table XV gives the average value of the factor by which the kinetic energy, as obtained from proton range-energy tables, must be multiplied for different particles.

We have

$$E_x = E_p\,(r)\,t_x, \tag{24}$$

with

E_x = kinetic energy of particle x

$E_p\,(r)$ = kinetic energy for a proton of range r as obtained from range-energy tables.

t_x = average value of multiplication factor (see Table XV).

Since it is actually impossible to know which prongs are actually due to which particles, we decided to multiply the kinetic energy of some prongs by a correction factor k and to add to these prongs a corrected $\bar{Q}$ value. For these corrected prongs we have thus

$$E_{TCi} = k\,E_i + \bar{Q}_c, \tag{25}$$

with

E_{TCi} = corrected total energy for prong i

k = correction factor (see Table XIV)

E_i = kinetic energy of prong i in unmodified results

$\bar{Q}_c$ = corrected $\bar{Q}$ value (see Table XIV).

Table XIII. Proportion of p, d, t, ^{3}He, and α particles to be expected from neutron star in the emulsion as a whole.

E_n (MeV)	p (%)	d (%)	t (%)	^{3}He (%)	α (%)
20	84.8	2.8	1.0	1.7	9.8
100	84.3	2.5	0.8	1.8	10.6
160	85.6	2.3	0.6	1.4	10.1
220	85.3	2.6	0.6	1.3	10.2
300	86.8	2.7	0.5	1.2	8.9

Table XIV. Values of multiplication factor k and of $\overline{Q}_c$ as a function of incident energy.

E_n (MeV)	p (%)	d (%)	t (%)	^{3}He (%)	α (%)	k	$\overline{Q}_c$ (MeV)
20	83.9	3.0	1.1	1.8	10.2	1.36	8.58
100	82.7	2.7	0.9	2.0	11.6	1.41	8.66
160	82.7	2.8	0.7	1.7	12.2	1.42	8.63
220	82.2	3.1	0.7	1.6	12.4	1.42	8.66
300	81.9	3.7	0.7	1.6	12.1	1.42	8.70

Equation (25) applies to all black prongs (except hammer tracks), and to all black-grey and grey-black prongs stopping in the emulsion. For the other prongs (all grey, and all black-grey and grey-black not stopping in the emulsion) we have

$$E_{Ti} = E_i + \bar{Q} \tag{26}$$

with

$\bar{Q}$ = average Q value for a proton in the emulsion as a whole (see Table XI).

For the prongs to which Eq. (26) applies, there is no difference between the "unmodified results" and the "modified" ones. In other words, these prongs are considered to be actually protons. The reasons for this distinction are:

1. For all black-grey, grey-black, and grey prongs not stopping in the emulsion, the residual range R_d as defined by Eq. (20) is obtained from the proton calibration track.

2. The very few grey prongs stopping in the emulsion have such long ranges that they are most probably protons.

Remember that the residual range $\bar{R}$ [see Eq. (22)] for black prongs not stopping in the emulsion was not obtained from the proton calibration track.

In order to obtain numerical values for k and Q_c, we proceeded in the following way.

From data of Table XIII, and with the number of prongs already assumed to be protons (grey, black-grey, and grey-black not stopping in the emulsion taken into account, new values of the percentages of protons, deuterons, tritons, ^{3}He, and α particles to be expected are computed (see Table XIV).

We have then

$$k = \frac{(P \times t_p) + (d \times t_d) + (t \times t_t) + (He^3 \times t_{He3}) + (\alpha \times t_\alpha)}{100} \tag{27}$$

with

t_p, t_d, t_t, t_{He3}, t_α : multiplication factor t as given in Table XV. The subscripts refer to the particle considered.

Table XV. Values of t (average value by which the proton's kinetic energy is to be multiplied for other kinds of particles).

Particle	t
p	1
d	1.3
t	1.45
^{3}He	3.4
α	4

p, d, t, ^{3}He, α : percentage of the different particles as given by Table XIV.

Similarly

$$\bar{Q}_c = \frac{(p \times \bar{Q}_p) + (d \times \bar{Q}_d) + (t \times \bar{Q}_t) + (^3He \times \bar{Q}_{^3He}) + (\alpha \times \bar{Q}_\alpha)}{100} \quad (28)$$

with

p, d, t, ^{3}He, α as defined in Eq. (27)

$\bar{Q}_p$, $\bar{Q}_d$, $\bar{Q}_t$, $\bar{Q}_{^3He}$, $\bar{Q}_\alpha$: the average Q value as given in Table XI. The subscripts refer to the particle considered.

IV. RESULTS

A. Size of Stars and Prong Distribution

Most of the data available on neutron stars are given in terms such as average number of prongs per star, distribution of prongs in angle, and darkness. In all tables and figures from this chapter, results for emulsion 1 and 2 (E_n = 220 MeV) are combined. For results with E_n = 20 MeV, see Sec. IV. D.

Table XVI gives as a function of E_n, (a) the number of stars scanned, (b) the total number of prongs, (c) the average number of prongs per star, and (d) the distribution of (b) and (c) among the different classes of prongs.

The average number of prongs per star, usually used as a criterion by which the incident energy is estimated, seems to give no significant results in the energy range we are interested in, although the average number of total prongs per star apparently increases slightly with increasing incident energy.

As far as black, black-grey, and grey-black prongs are concerned, no great changes appear under different bombarding conditions. The only discriminating feature seems to be the increasing proportion of grey prongs when E_n increases. This increase is very well marked and seems beyond any statistical error. Table XVII gives the number and percentage (within each class) of prongs of each class stopping and not stopping in the emulsion.

With the implicit assumption made in this work, that with the exception of black prongs the average kinetic energy of prongs for a given class will be roughly independent of the incident neutron energy, the repartition within a given class into stopping and not stopping prongs should depend only on the emulsion's dimensions. [This assumption is a direct consequence of assumption 11 (see Sec. II. E).] Since all emulsions are of the same dimensions we should expect the percentages to be roughly the same within statistical errors. This is the case as can be seen from Table XVII, but we feel that although our implicit assumption may be justified for black-grey and grey-black prongs, for grey prongs the justification becomes poor.

Table XVI. Number of stars scanned and number of prongs of each class.

E_n (MeV)		S	T	B	BG	GB	G	L
20	No.	559	1910	1744	130	30	5	1
	%		100	91.3	6.8	1.6	0.3	
	A		3.42	3.12	0.23	0.06	0.01	
100	No.	778	2125	1797	177	96	52	3
	%		100	84.6	8.3	4.5	2.4	
	A		2.73	2.31	0.23	0.12	0.07	
160	No.	684	1908	1411	224	157	113	3
	%		100	73.9	11.7	8.2	5.9	
	A		2.79	2.06	0.33	0.23	0.17	
220	No.	1392	4393	3226	508	234	421	4
	%		100	73.4	11.6	5.3	9.6	
	A		3.16	2.32	0.36	0.17	0.31	
300	No.	594	1940	1211	308	126	294	1
	%		100	62.4	15.9	6.5	15.2	
	A		3.27	2.04	0.52	0.21	0.50	

E_n = neutron's incident energy A = average number per star B = black prongs

BG = black-grey prongs G = grey prongs GB = grey-black prongs

L = hammer tracks (^{8}Li) S = number of stars scanned T = total prongs

Table XVII. Number and percentage of prongs not ending in the emulsion arranged according to class.

E_n (MeV)		B_1	B_2	BG_1	BG_2	GB_1	GB_2	G_1	G_2
	No.	1726	18	59	71	4	26	--	5
20	%	99.0	1.0	45.4	54.6	13.3	86.7	--	100
	No.	1572	225	110	67	24	72	--	52
100	%	87.5	12.5	62.1	37.9	25.0	75.0	--	100
	No.	1156	255	128	96	44	113	3	110
160	%	82.0	18.0	57.0	43.0	28.0	72.0	2.7	97.3
	No.	2631	595	319	189	59	175	1	420
220	%	81.6	18.4	62.8	37.2	25.2	74.8	0.2	99.8
	No.	984	227	175	133	41	85	--	294
300	%	81.3	18.7	56.8	43.2	32.5	67.5	--	100

E_n = neutron's incident energy

% refers to the total percentage of prongs of the class

B = black

Subscript 1 = stopping in the emulsion

Subscript 2 = not stopping in the emulsion

BG = black-grey

GB = grey-black

G = grey

Unfortunately, the data available on grey prongs give no hint as to what is to be believed, because the effect of the incident energy on the average energy of grey prongs is completely masked by the small sizes of the emulsion (3 in. by 1 in. by 600 μ). Too few grey prongs stopping in the emulsion are available to confirm or contradict this hypothesis.

The distribution of black prongs more or less confirmed the results for $\overline{R}$ (see Table IV).

Table XVIII gives the number and percentage (with respect to the total number of stars) of stars that had a black prong and were rejected as being possibly an unidentified recoil nucleus. According to some authors,[12,13] the existence of such a short black track is a criterion that distinguishes light- and heavy-nuclei groups as target nuclei.

In most cases, the threshold energy for a star-type reaction is higher for heavy-group-target nuclei than for light-group-target nuclei. As may be seen in Tables VI to IX, the proportion of star-type reactions due to heavy-group nuclei increases slightly with increasing E_n (see value for f). We should thus expect the percentage of stars with residual nuclei to decrease with increasing incident energy.

This doesn't seem to be the case, however. We think that the usefulness of the results of Table XVIII is very poor, because during the scanning job, we emphasized the "less than 10 microns" criterion more than the "very black" one (see assumption 8). The length criterion is an objective one, whereas the blackness criterion is a rather subjective one.

Figures 7 through 10 show the number of stars N (after normalization in percent) versus the number of prongs n for the different E_n. Here again, a slight displacement of the peak to the right (more prongs) appears, showing, in a not too convincing way, that the number of prongs increases with the incident energy.

B. Average Visible Energy per Star and Its Distribution*

Table XIX shows the value of $\overline{E}_v$ for both modified and unmodified results. We define $\overline{E}_v$ as the average visible energy per star, i.e.,

*For results with $E_n = 20$, see Sec. IV.D.

Table XVIII. Number and percentage of stars that had a black track and were rejected as being an unidentified residual nucleus.

E_n (MeV)	Number	Percentage
20	124	22.2
100	371	47.7
160	235	34.4
220	650	46.7
300	359	60.4

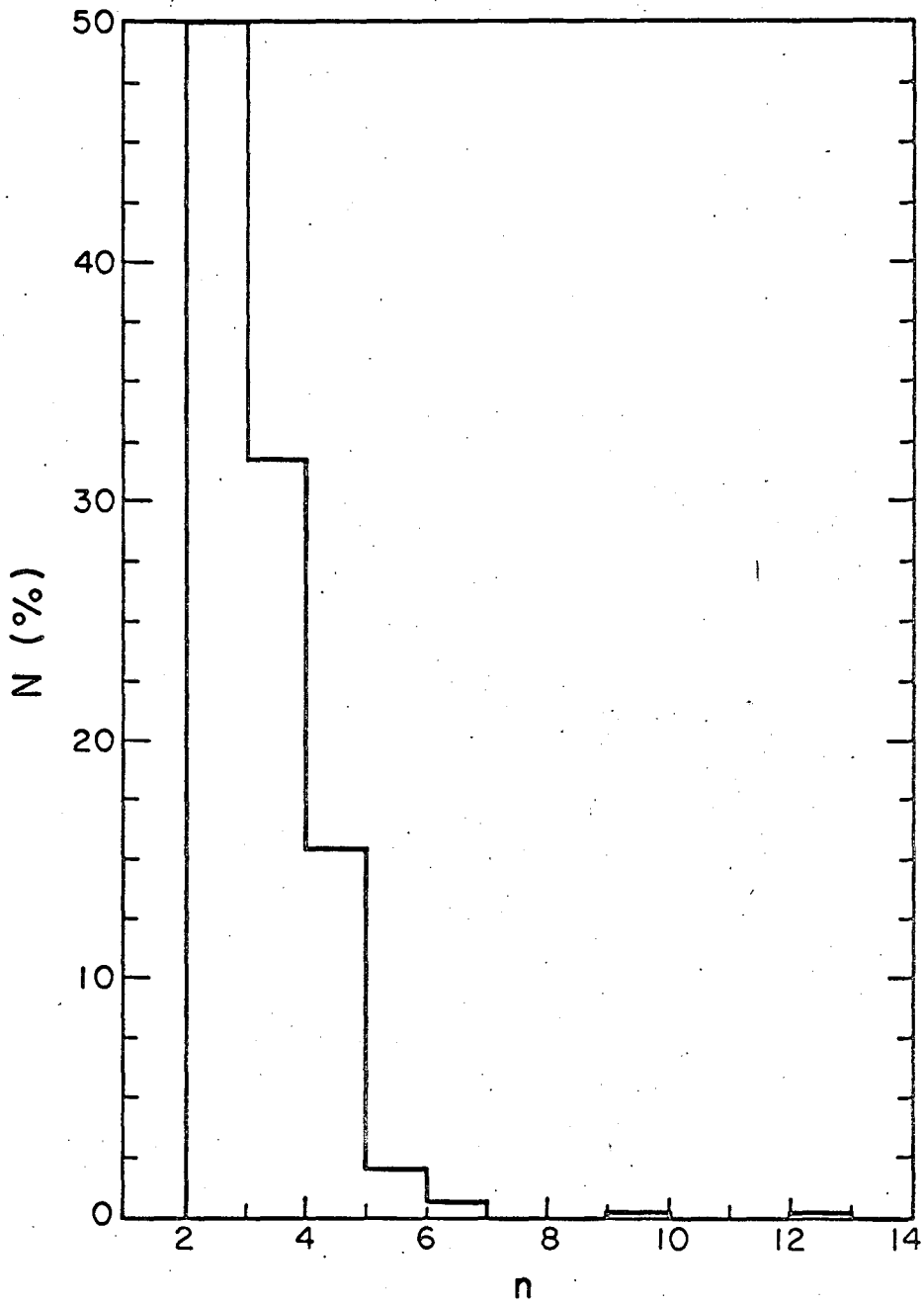

MU-36544

Fig. 7. Normalized number of stars N with n prongs. E_n = 100 MeV.

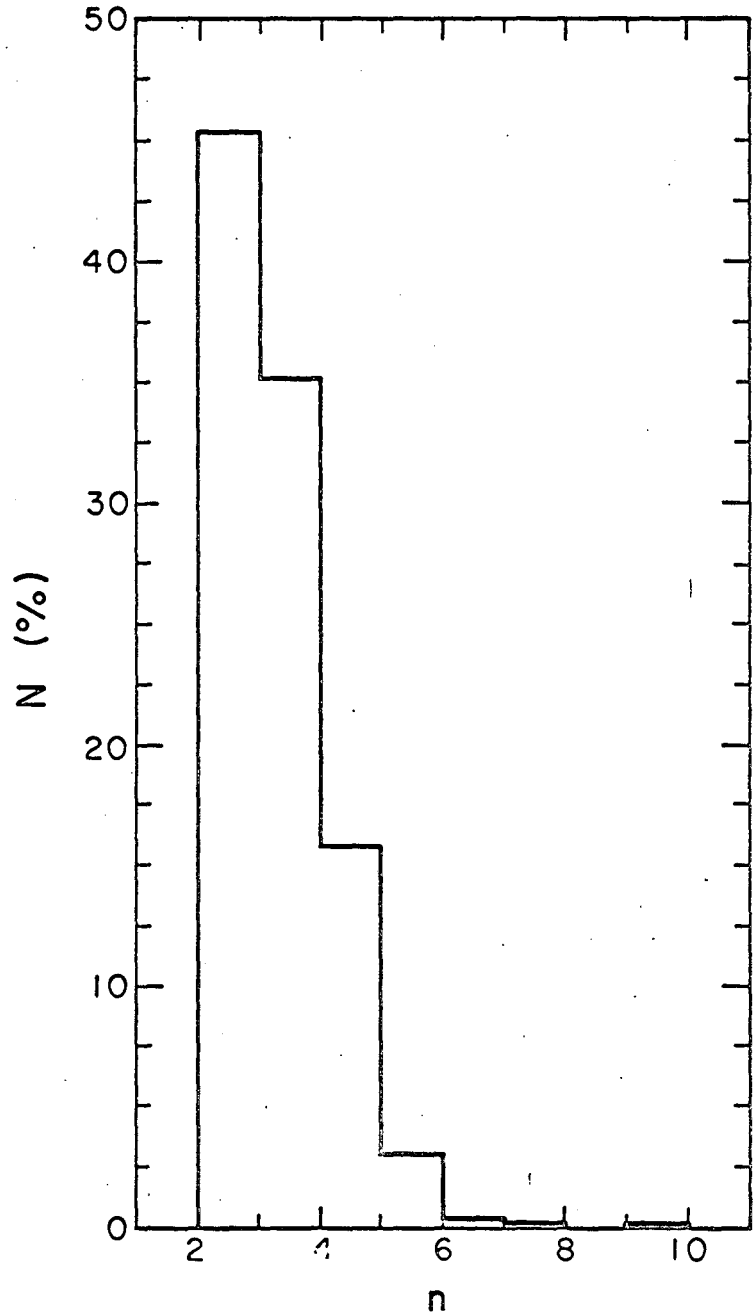

MU-36545

Fig. 8. Normalized number of stars N with n prongs. E_n = 160 MeV.

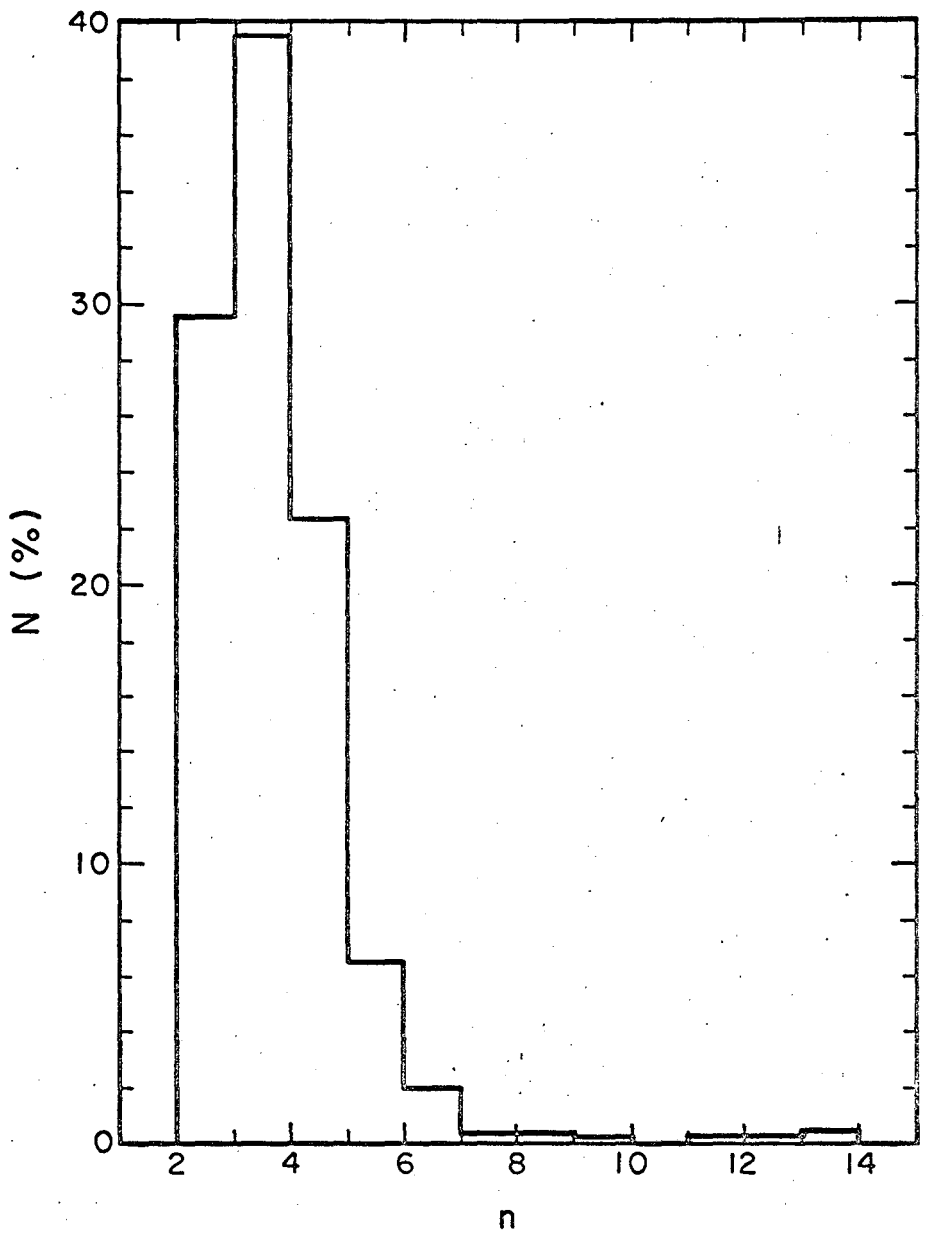

MU-36543

Fig. 9. Normalized number of stars N with n prongs. E_n = 220 MeV.

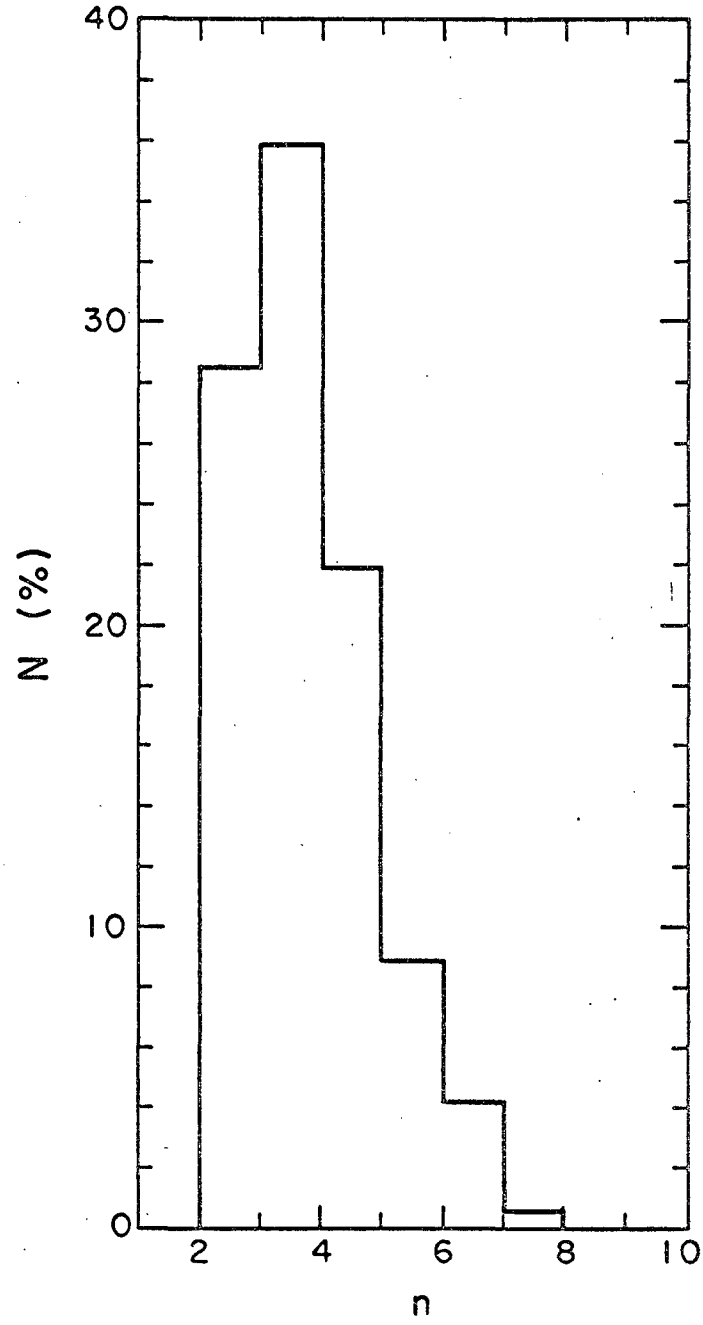

MU-36546

Fig. 10. Normalized number of stars N with n prongs. E_n = 300 MeV.

Table XIX. Values of $\bar{E}_v$ and its distribution.

E_n (MeV)			$\bar{E}_v$	E_1	E_2	E_3	E_4	Q	$\bar{E}_v/E_n$ (%)
20	A	MeV	38.9	10.1	6.6	2.9	0.6	28.8	194.5
		%	100	26.0	17.0	7.5	1.5	74.0	
	B	MeV	41.8	12.6	9.0	3.0	0.6	29.2	209.0
		%	100	30.1	21.5	7.2	1.4	69.9	
100	A	MeV	42.2	18.8	8.4	6.5	3.9	23.4	42.2
		%	100	44.6	19.9	15.5	9.2	55.4	
	B	MeV	47.0	23.3	11.8	7.6	3.9	23.7	47.0
		%	100	49.5	25.2	16.0	8.3	50.5	
160	A	MeV	54.0	30.1	10.4	10.2	9.5	23.9	33.8
		%	100	55.7	19.2	18.9	17.6	44.3	
	B	MeV	59.8	35.7	14.7	11.5	9.5	24.1	37.4
		%	100	59.7	24.6	19.2	15.9	40.3	
220	A	MeV	64.7	37.6	10.5	9.4	17.7	27.1	29.4
		%	100	58.1	16.2	14.5	27.4	41.9	
	B	MeV	71.0	43.7	15.0	11.0	17.7	27.3	32.3
		%	100	61.5	21.1	15.5	24.9	38.5	
300	A	MeV	77.0	49.0	10.7	10.2	28.1	28.0	25.7
		%	100	63.6	13.9	13.2	36.5	36.4	
	B	MeV	83.1	54.8	15.2	11.5	28.1	28.3	27.7
		%	100	65.9	18.3	13.8	33.8	34.1	

E_1 = average kinetic energy per star
E_2 = average kinetic energy per star due to prongs stopping in the emulsion
E_3 = average kinetic energy per star due to prong not ending in the emulsion excepted grey ones
E_4 = average kinetic energy per star due to grey prong not ending in the emulsion
Q = average Q value per star
A = unmodified results (all prongs protons)
B = modified results (after correction; ,see Sec. III. F)

$$\overline{E_v} = \frac{\sum_{i}^{n} E_{vi}}{n} \tag{29}$$

with E_{vi} = visible energy of star i

n = total number of stars scanned as a function of E_n.

These $\overline{E}_v$ have been split into different components, which are;

E_1 = average kinetic energy per star

E_2 = average kinetic energy per star due to prongs stopping in the emulsion

E_3 = average kinetic energy per star due to all prongs (except the grey ones) not stopping in the emulsion

E_4 = average kinetic energy per star due to grey prongs not stopping in the emulsion.

We have

$$E_1 = E_2 + E_3 + E_4 \tag{30}$$

$$\overline{E}_v = E_1 + Q, \tag{31}$$

with Q = average Q value per star.

1. Unmodified Results (All Prongs Are From Protons)

A net increase of $\overline{E}_v$ appears for increasing incident energy, providing thus a good discrimination between the different bombarding conditions. The influence of E_4 on that increase is predominant. There is also a slight increase of Q (E_n), which is a direct consequence of the variation of the average number of prongs per star and the $\overline{Q}$ values of Table XI as a function of E_n.

However, the contribution of Q to $\overline{E}_v$ decreases very significantly with increasing incident energy.

2. Modified Results

The importance of E_4 is slightly decreased here, as may be expected from the way the modified results were obtained (see Sec. III. F). Even in this case, the increase of both $\overline{E}_v$ and E_4, with increasing E_n, remains very apparent.

In the last column of Table XIX the ratio $\overline{E}_v/E_n$ is given in percent. As may be seen, the percentage of visible energy decreases very significantly when E_n increases. This seems to prove that, as

the incident neutron energy increases, the amount of energy carried away in invisible form (mostly neutrons) becomes more and more important.

However, such a conclusion depends strongly on the validity of our implicit assumption (average energy of fast prongs independent of incident energy).

C. Distribution of Stars in 10-MeV Intervals

Figures 11 through 14 show the number of stars after normalization (N in percent) versus the visible energy released (E in 10-MeV intervals) for both modified and unmodified results.

In these figures, the unmodified results have been displaced to the right for clarity.

In all four cases, although a peak in the 30-MeV interval appears, its amplitude decreases with increasing incident energy. The increase of incident energy seems to produce an erasure of the 30 to 40 MeV interval peak and an enhancement of the high-energy tail.

As may be expected from the definition of the correction factor k and of $\overline{Q}_c$ (see Sec. III. F), no great distortion of the spectrum appears between the modified results and the unmodified ones.

The overall effect is more or less a "heating" of the spectrum in the modified case.

In Figs. 11 and 12 (E_n = 100 MeV and E_n = 160 MeV), a few stars have a visible energy probably too high to belong to the spectrum, and we believe that they are due to some background (cosmic rays). Because of their rarity, they have no preceptible effect on $\overline{E}_v$ and were thus not disregarded in the computation of $\overline{E}_v$.

The poor discrimination, for that range of incident energy, existing in the average number of prongs per star provides an explanation for the existence of a 30- to 40-MeV interval peak in each case.

Most of the stars from the 30- to 40-MeV interval belong to the 2 to 3 black-prong stars, which corresponds to the most numerous class of n-prong stars (over 50% of all the stars in the less favorable case).

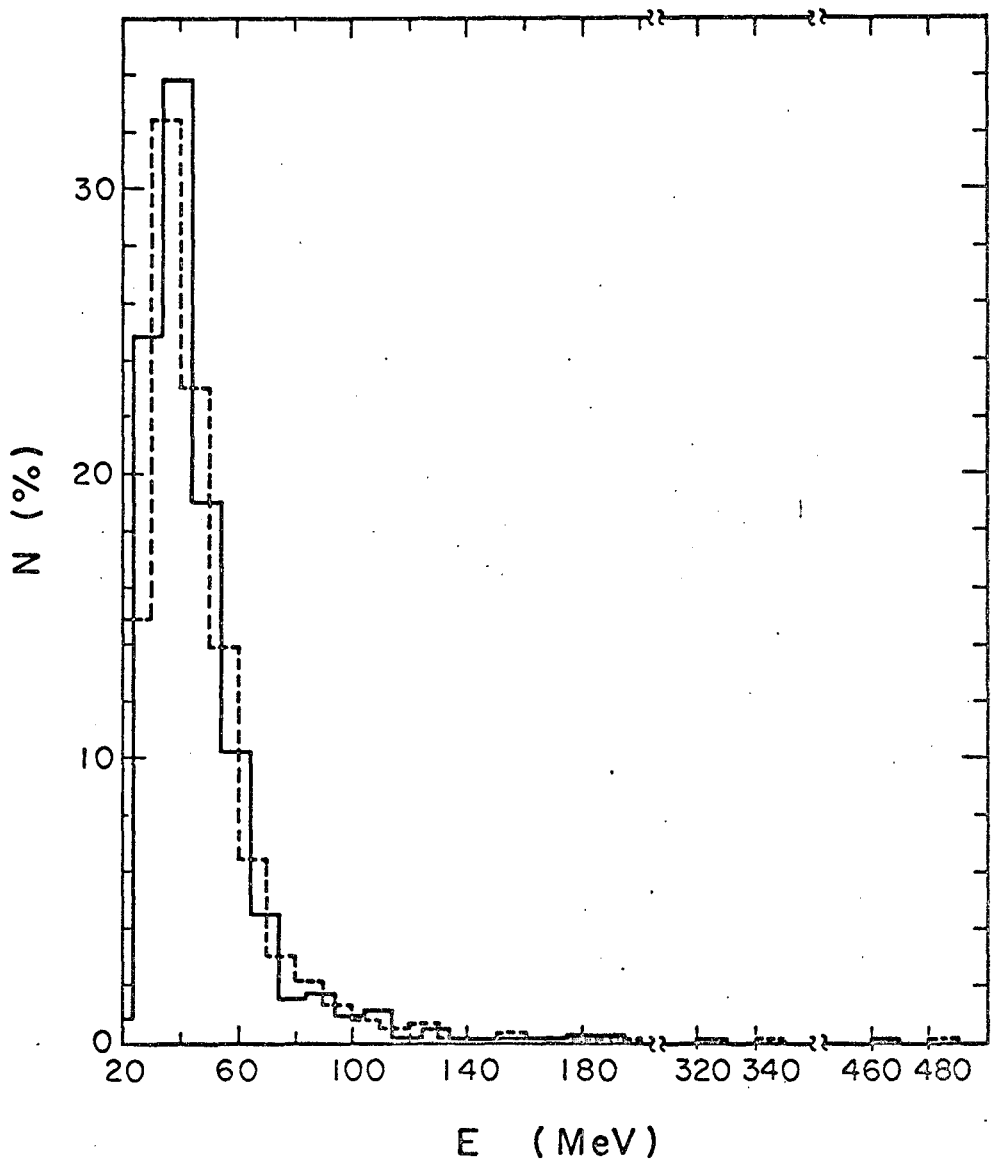

MU-36541

Fig. 11. Normalized number of stars N with visible energy in 10-MeV interval for E_n = 100 MeV.
Solid line: unmodified results. Dashed line: modified results. The unmodified results are displaced to the right for clarity.

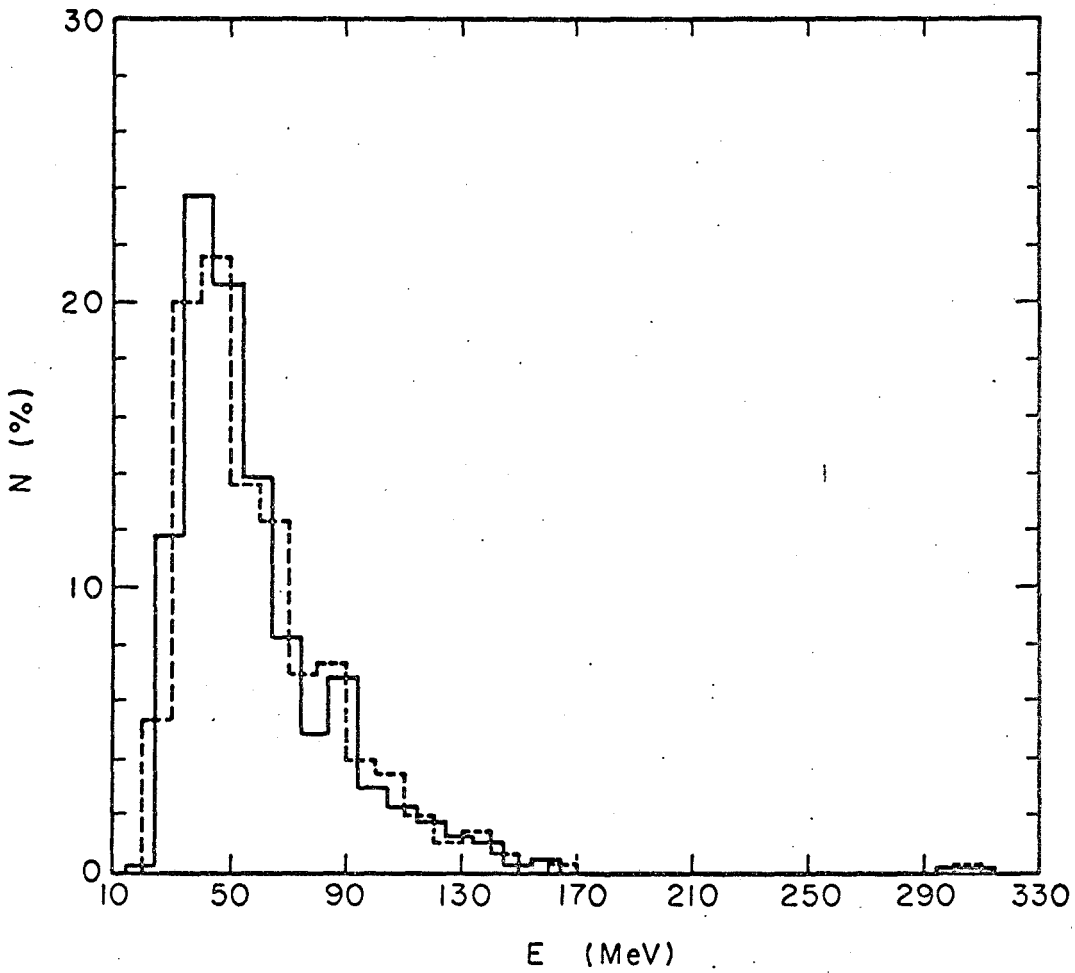

MU-36540

Fig. 12. Normalized number of stars N with visible energy in 10-MeV interval for E_n = 160 MeV.
Solid line: unmodified results. Dashed line: modified results. The unmodified results are displaced to the right for clarity.

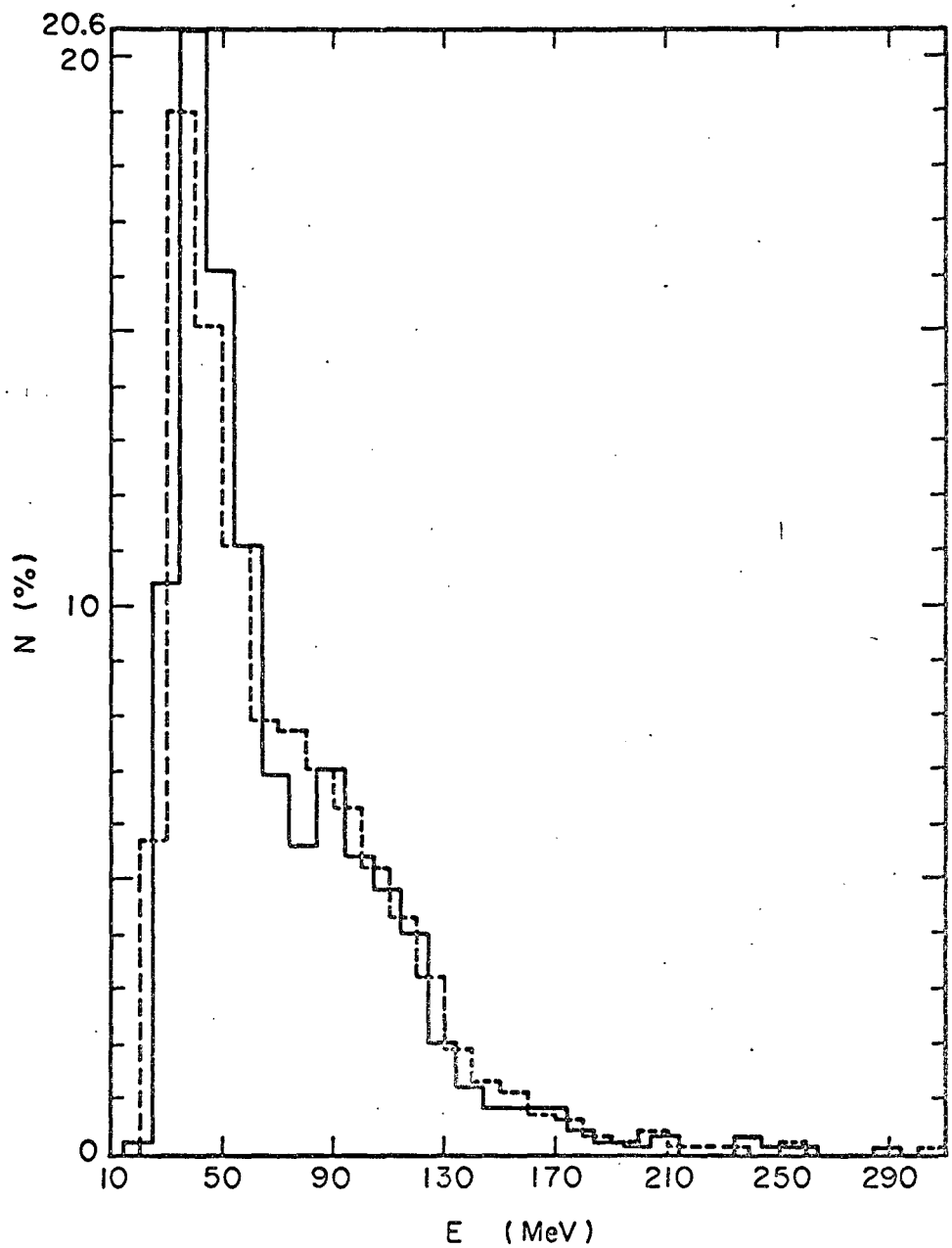

MU-36539

Fig. 13. Normalized number of stars N with visible energy in 10-MeV interval for E_n = 220 MeV.
Solid line: unmodified results. Dashed line: modified results.
The unmodified results are displaced to the right for clarity.

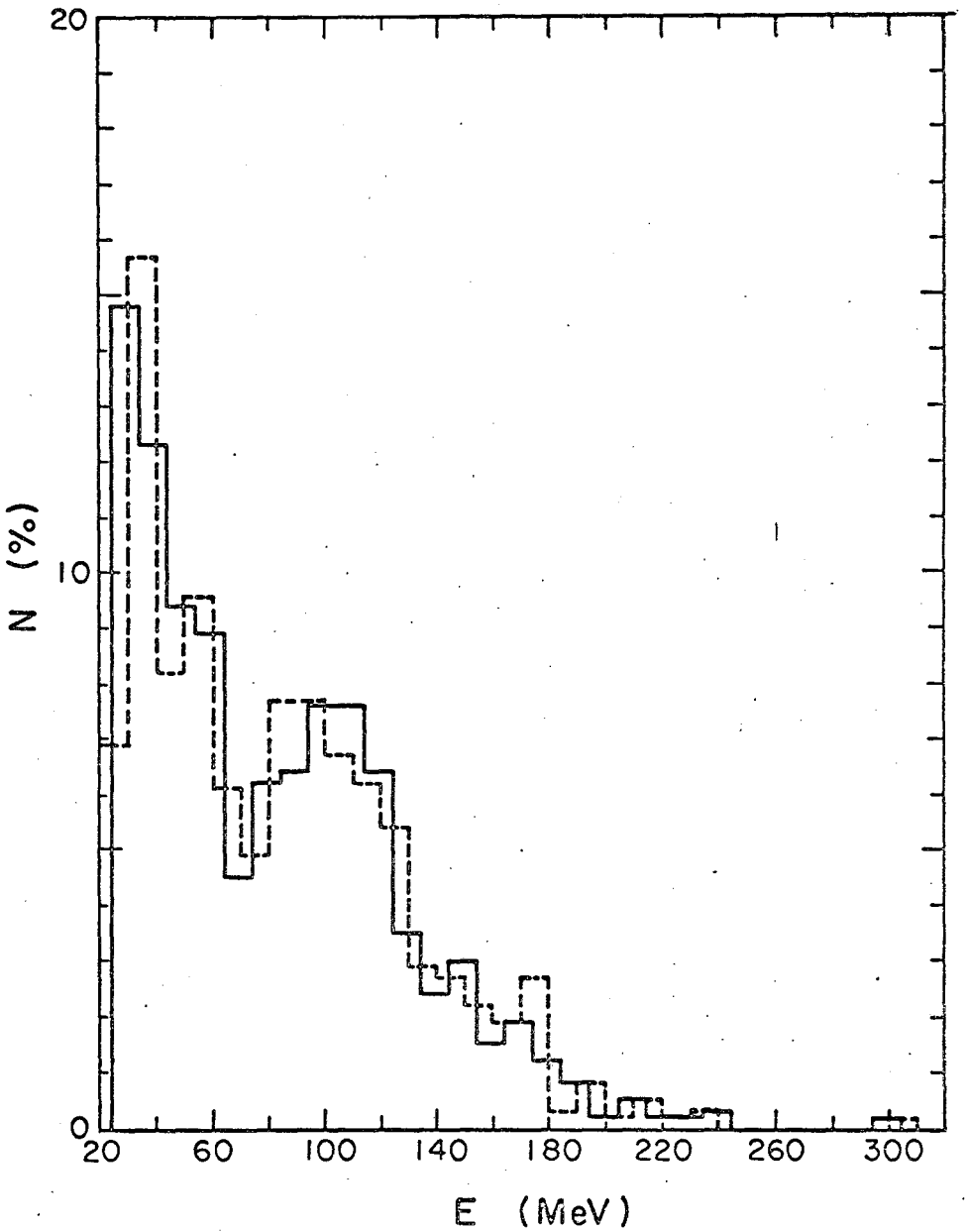

MU-36542

Fig. 14. Normalized number of stars N with visible energy in 10-MeV interval for E_n = 300 MeV.
Solid line: unmodified results. Dashed line: modified results.
The unmodified results are displaced to the right for clarity.

D. Results for E_n = 20 MeV

1. Star Sizes and Prong Distribution

As Table XVI shows, the average number of prongs per star is not in accordance with the results obtained for the other incident energies.

One striking fact that appears clearly in Fig. 15 is the existence of a peak in the 4-prong region, although we should rather expect a peak in the 2 to 3-prong region.

On the other hand, the main conclusion of Sec. IV.A (increasing number of grey prongs for increasing E_n) remains valid.

Table XVII shows no unusual discrepancy between this case and those for other E_n's; the decreases in the percentage of black-grey and grey-black prongs ending in the emulsion are probably due to greater statistical errors.

2. Average Visible Energy per Star and Its Distribution

The value obtained for $\overline{E}_v$ shows that, in this case, the method leads to an impossibility (twice as much outgoing energy as the incoming one). See also Table XIX.

As far as E_4 is concerned, no discrepancy existed between this result and those for other E_n's; this is also true for E_2 and E_3.

At first glance, Q seems to be responsible for the impossible $\overline{E}_v$ value; the high value of Q is a direct consequence of the 4-prong-star peak of Fig. 15.

3. Reasons for the Failure of the Star Method

a. Assumption 2 (see Sec. II.E) becomes very poor, as all star processes are threshold reactions; it is mostly the high-energy tail of the neutron spectrum given in Fig. 1 that will provide neutrons to produce star-type reactions. The average energy of star-producing neutrons is more likely 2 to 3 times 20 MeV in this case.

b. The σ_{in} values for E_n = 20 MeV (see Table VI) were actually obtained from extrapolation, and we believe that they are much too high, especially for heavy-target-nuclei group. This leads to a wrong value of $\overline{Q}$ (see Table XI) that is probably too high.

c. Assumption 1 (see Sec. II.E) probably becomes very poor with the small amount of energy available; the probability that enough energy is left to eject a neutron after ejection of at least 2 other visible particles (see assumption 10) should not be very great.

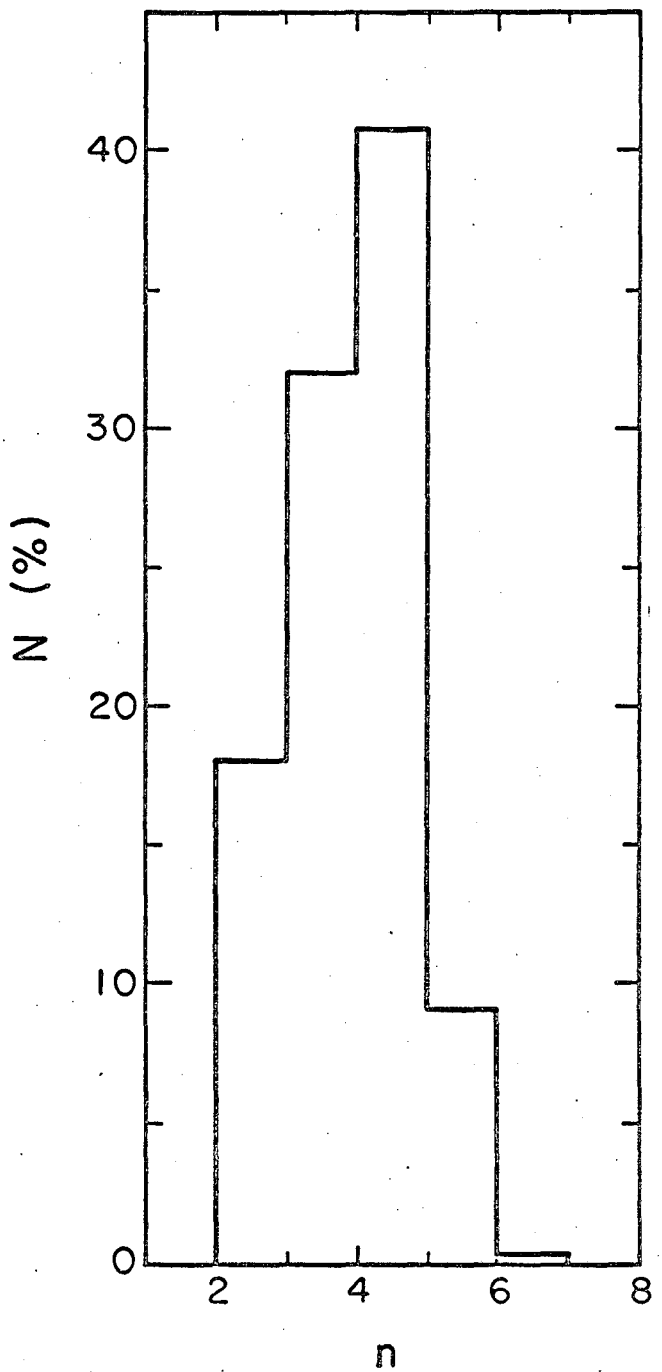

MU-36536

Fig. 15. Normalized number of stars N with n prongs. E_n = 20 MeV.

These arguments seem to be a logical explanation for the failure of the star method as far as $\overline{E}_v$ is concerned. However, this does not explain why the average number of prong per star is so high and why there is a 4-prong-star peak in Fig. 15.

4. Possible Explanation of the High Average Number of Prongs per Star

We should think that assumption 10 (see Sec. II. E) could also introduce a larger error for smaller E_n than for a larger one. This argument is mostly intuitive and is contradicted by the existence of the 4-prong-star peak in Fig. 15.

Table XVI shows that the high value of the average number of prongs per star for $E_n = 20$ MeV is due to the high average number of black prongs per star. So it seems that incident neutrons with energy around 20 MeV produce star-type reactions mostly with light-nuclei-group elements (C, N, S, O), which require much less energy in Q form for the ejection of a particle than with elements of the heavy-nuclei group (Ag, Br, I).

In that case, there seems to be a tendency to use the available energy to eject many particles with little kinetic energy rather than a few particles with greater kinetic energy.

When the incident energy increases, the portion of stars due to heavy-nuclei-group disintegration becomes more and more important, requiring, on the average, more and more energy to provide the Q-form energy associated with each outgoing particle.

This tends to reduce, for a while, the average number of prongs per star until the incident energy is high enough that the proportion of star events due to heavy-nuclei-group disintegrations remains crudely constant. This last state seems to be reached when $E_n = 100$ MeV.

A further increase in incident energy appears in kinetic-energy form rather than in an increase of the number of prongs. This interpretation is confirmed by the results obtained for the incident energy range 100 to 300 MeV, but it is still not much more than a guess. In order to have some validity it should require a confirmation for incident neutron energy below 100 MeV.

The existence of the 4-prong-star peak in Fig. 15 could also be explained by the disintegrations of oxygen nuclei into 4 α particles.

This last reaction requires practically no energy in the Q form. However, the value of $\overline{R}$ (40 microns) corresponds to α particles with 8-MeV kinetic energy, which tends to prove that the average neutron incident energy is 40 or 60 MeV rather then 20 MeV.

5. Distribution of Stars in 10-MeV Intervals

Figure 16 shows the normalized number of stars versus the visible energy released for E_n = 20 MeV. No discrepancy appears between these results and those for other E_n's and the conclusion of Sec. IV.C remains valid in this case.

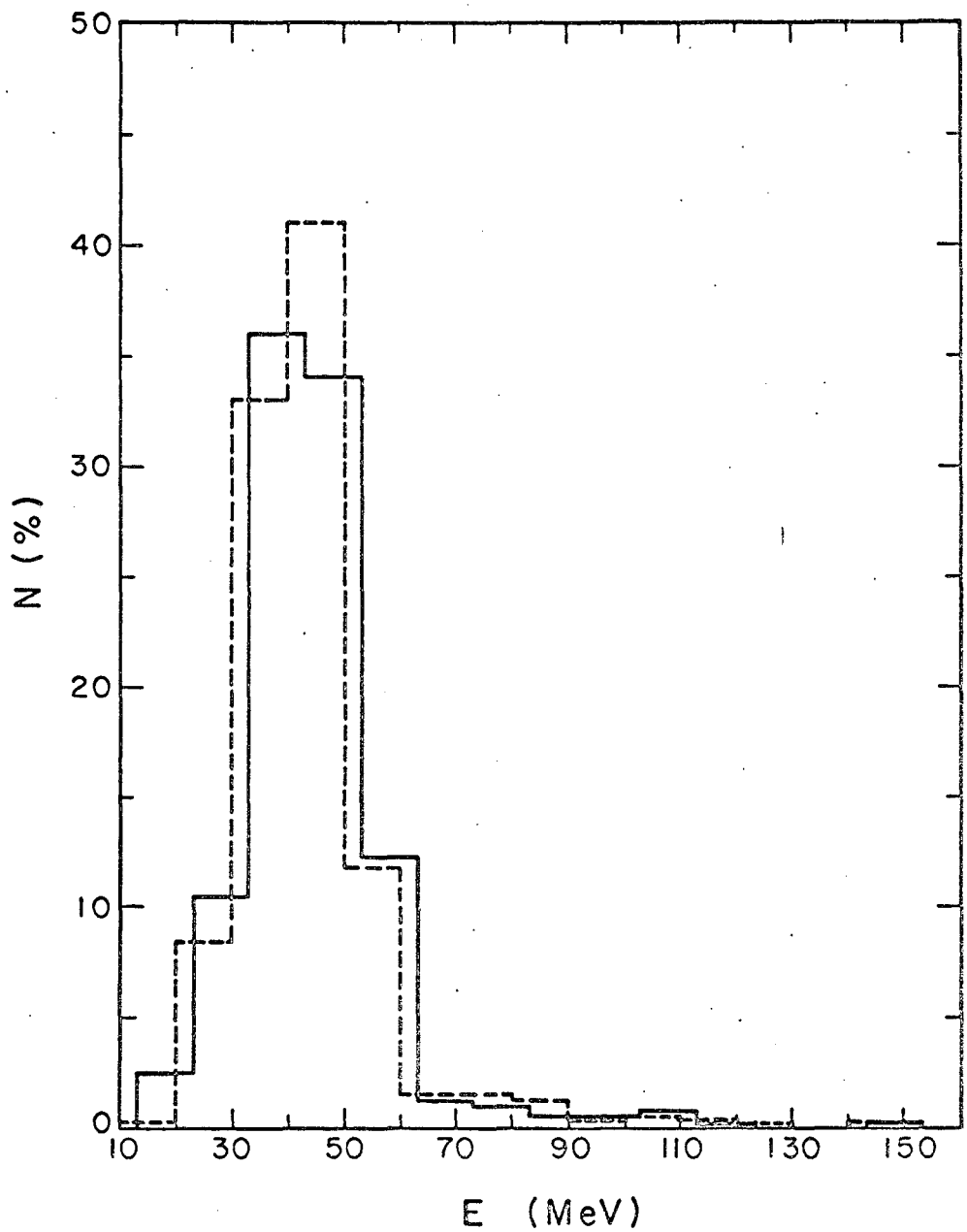

MU-36537

Fig. 16. Normalized number of stars N with visible energy in 10-MeV interval for E_n = 20 MeV.
Solid line: unmodified results. Dashed line: modified results.
The unmodified results are displaced to the right for clarity.

V. CONCLUSIONS

The obtainment of an accurate value for $\overline{E}_v$ as a function of E_n (see Eq. 29) seems to depend almost entirely on an accurate estimation of the kinetic energy of grey prongs leaving the emulsion (see E_4 in Table XIX). In that respect assumption 11 is the weakest point of the method. Assumption 11 implies that the average energy of grey prongs is independent of neutron incident energy, since the same residual range is added to grey prongs leaving the emulsion for all E_n's.

The accuracy of results for $\overline{E}_v$ (see Table XIX) should not be trusted without a check on the validity of assumption 11.

Since this work was done in order to find some useful results for neutron spectroscopy purposes, we were more interested in a good discrimination between the different bombarding conditions than in an accurate value of $\overline{E}_v$.

During this work, the a-priori knowledge of the bombarding neutron spectrum (see Sec. III. A) could destroy any usefulness of the results for neutron spectroscopy purposes. In that respect, assumption 11 was a necessary thing, since it prevents any drastic change in the treatment of the data from one bombarding condition to another.

It is our opinion that a good discrimination was obtained, during this work, for the value of $\overline{E}_v$ as the function of the neutron average incident energy in the range from 100 to 300 MeV (see Sec. IV. B and Table XIX).

We believe that if assumption 11 turns out to be very poor, the changes in $\overline{E}_v$ results can occur only in a favorable way (better discrimination between the different bombarding conditions).

The results obtained during this work do not permit the reconstruction of an unknown neutron spectrum. But we believe that this method can be used to obtain a good estimation of the average neutron incident energy.

However, the tremendous number of man-hours involved in the use of this method reduces its usefulness at this time.

A rather unexpected factor provides a much simpler way to reach the same goal. Although the average number of prongs per star makes possible a very poor discrimination between the different bombarding

conditions, this is not the case for the average number of grey prongs per star (see Table XVI and Fig. 17).

Moreover, if this last factor is used as a discrimination criterion for neutron spectroscopy purpose, the method will simplify in such a way that it will become practical.

In that case, as assumptions (except 2, 9, and 10, see Sec. II. E) are not needed anymore, and above all, the accuracy of assumption 11 does not matter anymore.

With this simplified method, all that has to be done is simply to count the number of stars together with the number of grey prongs, saving in that way a tremendous part of the scanning job (see Sec. III. B).

As can be seen in Table XVI, if the average number of grey prongs per star is chosen as a criterion to obtain the average neutron incident energy of an unknown bombarding neutron spectrum, a discrimination can even be obtained for E_n below 100 MeV (see Fig. 17).

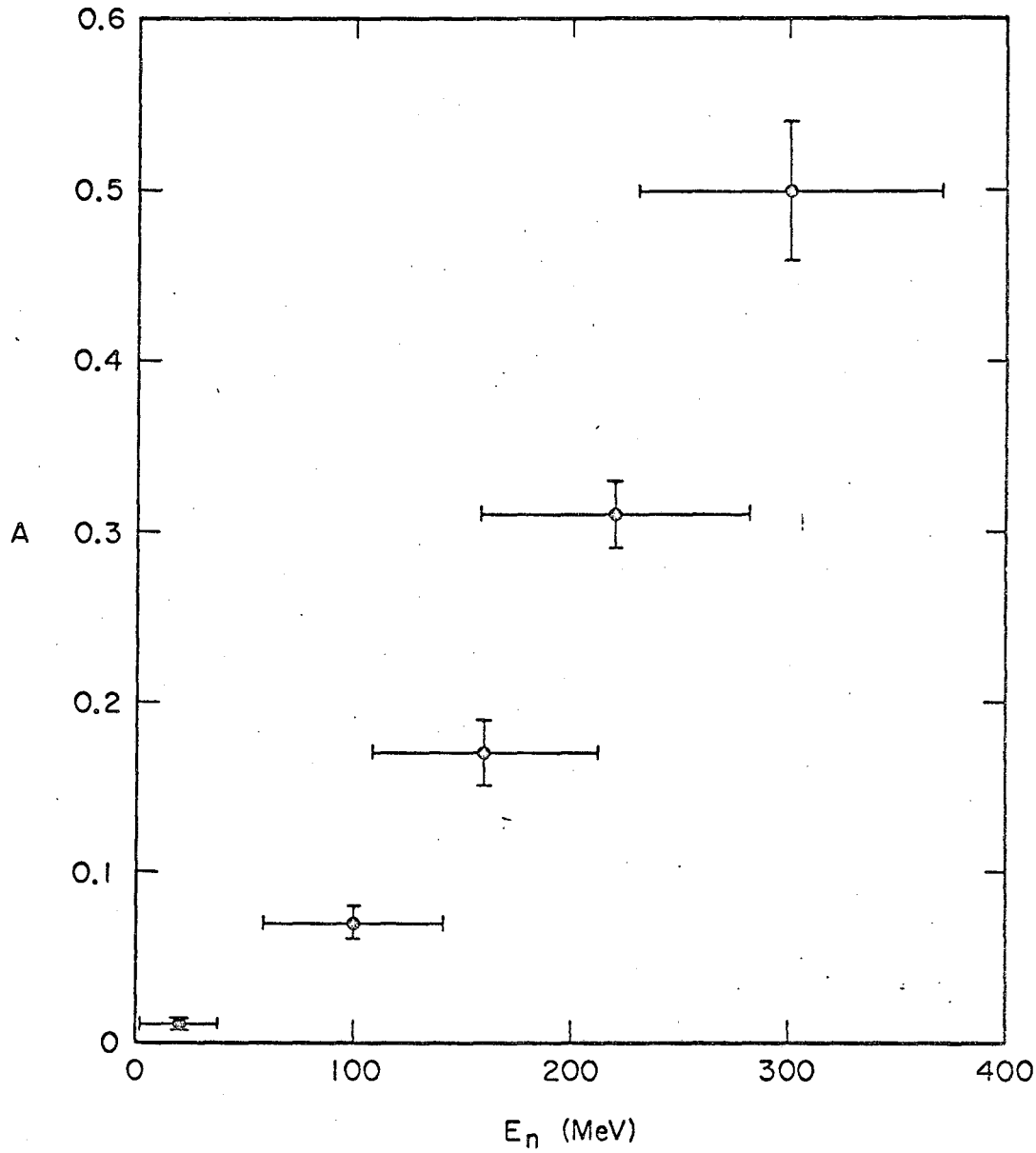

MU-36583

Fig. 17. Average number of grey prongs per star A versus incident neutron average energy E_n.
Errors shown in A are statistical errors due to counting.
Errors shown in E_n are values of $\Delta E_{1/2}$ (see Eq. 16).

ACKNOWLEDGMENTS

The author wishes to thank Dr. Roger Wallace for suggesting the problem and for his constant encouragement and guidance during this work.

He would like to thank also Dr. Harry Heckman for many helpful discussions and for providing the scanners.

Thanks are also due to Mrs. Sonia Vardas and Mr. Stanley Ding for their skillful scanning work, to Mr. Barry Howard for the programming, and to the crews of the 184-inch and 88-inch cyclotrons.

This work was performed under the auspices of the U. S. Atomic Energy Commission.

REFERENCES

1. Walter Barkas, Nuclear Research Emulsions, Vol. 1 (Academic Press, New York and London, 1963).
2. P. Demers, Ionographie - Les Emulsions Nucleaires - Principes et Applications, (Presses Universitaires de Montreal, 1958).
3. William H. Sullivan, Trilinear Chart of Nuclides, (1957), ORNL (no number).
4. R. Hildebrand, D. Hicks, W. Harker, Summary of Neutron Cross Section Measurements for 14 MeV to 280 MeV Neutrons, UCRL-1305, May 1951.
5. Walter Barkas and Martin Berger, Tables of Energy Losses and Ranges of Heavy Charged Particle, NASA SP-3013 (1964).
6. Walter Barkas, (private communication), 1965.
7. William Paul Ball, Nuclear Scattering of 300 MeV Neutrons, UCRL-1938, August 1952.
8. R. Serber, The Production of High Energy Neutrons by Stripping, Phys. Rev. 72, 1008 (1947).
9. R. Serber, Nuclear Reactions at High Energies, Phys. Rev. 72, 1114 (1947).
10. M. Goldberger, The Interaction of High-Energy Neutrons and Heavy Nuclei, Phys. Rev. 74, 1269 (1948).
11. V. Weisskopf, Statistics and Nuclear Reactions, Phys. Rev. 52, 295 (1937).
12. K. J. Le Couteur, The Evaporation Theory of Nuclear Disintegration, Proc. Phys. Soc. (London) A63, 259 (1950).
13. Niels Bohr, Neutron Capture and Nuclear Constitution, Nature 137, 344 (1936).
14. L. Evan Bailey, Angle and Energy Distributions of Charged Particles from the High-Energy Nuclear Bombardment of Various Elements (Ph. D. Thesis), UCRL-3334, March 1956.
15. W. D. Lock and P. V March, A Study of the Nuclear Disintegration Produced by 950-MeV Protons, Proc. Roy. Soc. (London) A231, 368 (1955).
16. Roger Wallace and Charles Sondhaus, Techniques Used in Shielding Calculations for High-Energy Accelerators: Applications to Space Shielding, UCRL-10436, October 1962.

This report was prepared as an account of Government sponsored work. Neither the United States, nor the Commission, nor any person acting on behalf of the Commission:

A. Makes any warranty or representation, expressed or implied, with respect to the accuracy, completeness, or usefulness of the information contained in this report, or that the use of any information, apparatus, method, or process disclosed in this report may not infringe privately owned rights; or

B. Assumes any liabilities with respect to the use of, or for damages resulting from the use of any information, apparatus, method, or process disclosed in this report.

As used in the above, "person acting on behalf of the Commission" includes any employee or contractor of the Commission, or employee of such contractor, to the extent that such employee or contractor of the Commission, or employee of such contractor prepares, disseminates, or provides access to, any information pursuant to his employment or contract with the Commission, or his employment with such contractor.